Ultrafast Infrared Spectroscopy in Biomolecules: Active Site Dynamics of Heme Proteins

JEFFREY R. HILL,[1] DANA D. DLOTT,[1,*] CHRIS W. RELLA,[2] TODD I. SMITH,[2] H. A. SCHWETTMAN,[2] KRISTEN A. PETERSON,[3] ALFRED KWOK,[4] K. D. RECTOR,[4] and M. D. FAYER[4]

[1]School of Chemical Sciences, University of Illinois at Urbana-Champaign, Box 37-1 Noyes Lab, 505 S. Mathews Ave, Urbana, Illinois 61801; [2]Hansen Experimental Physics Laboratory, Stanford University, Stanford, California 94305; [3]Department of Chemistry and Biochemistry, New Mexico State University, Las Cruces, New Mexico 88003; and [4]Department of Chemistry, Stanford University, Stanford, California 94305

SYNOPSIS

Rapid advances in the generation of intense tunable ultrashort mid-infrared (IR) laser pulses allow the use of ultrafast IR pump-probe and vibrational echo experiments to investigate the dynamics of the fundamental vibrational transition of CO bound to the active site of heme proteins. The studies were performed using a free-electron laser (FEL) and an experimental set up at the Stanford University FEL Center. These novel techniques are discussed in some detail. Pump-probe experiments on myoglobin-CO (Mb-CO) measure CO vibrational relaxation (VR). The VR process involves loss of vibrational excitation from CO to the protein and solvent. Infrared vibrational echoes measure CO vibrational dephasing. The quantum mechanical treatment of the force-correlation function description of vibrational dynamics in condensed phases is described briefly. A quantum mechanical treatment is needed to explain the temperature dependence of VR in Mb-CO from 10 to 300 K. A molecular-level description including elements of heme protein structure in the treatment of vibrational dynamics is also discussed. Vibrational relaxation of CO in Mb occurs on the 10^{-11}-s time scale. VR was studied in proteins with single-site mutations, proteins from different species, and model heme compounds. A roughly linear relationship between carbonyl stretching frequency and VR rate has been observed. The dominant VR pathway is shown to involve anharmonic coupling from CO through the π-bonded network of the porphyrin, to porphyrin vibrations with frequencies $> 400\ cm^{-1}$. The heme protein influences VR of bound ligands at the active site primarily via altering the through π-bond coupling between CO and heme. Preliminary vibrational echo studies of the effects of protein conformational relaxation dynamics on ligand dephasing are also reported.

INTRODUCTION

Because of the "fingerprint" nature of mid-infrared (IR) spectroscopy, and the widespread availability of extremely sensitive Fourier-transform IR spectrometers in the 2.5–25-μm range, IR has become a valuable tool in practically all chemical applications. The application of IR to studies of macromolecular dynamics[1] has not been as fruitful, because macromolecular vibrational spectra are usually so congested that the "fingerprint" of a macromolecule is "smudged." In the same way that multidimensional pulse experiments in nuclear magnetic resonance imaging (NMR)[2,3] have become powerful tools to study macromolecular structure and dynamics, new IR techniques ought to be developed to relieve the vibrational congestion of macromolecular spectra. The recent explosion of new developments in short-pulse, tunable coherent laser sources in the mid-IR will make these new techniques feasible. These new laser sources open up the possibilities of exploiting nonlinear or coherent optical interactions to obtain new information about the dynamical behavior of macromolecules.

In this article, we discuss experiments using

* To whom all correspondence should be addressed.

Biospectroscopy, Vol. 2, 277–299 (1996)
 CCC 1075-4261/96/050277-23

time-resolved IR spectroscopies to study molecular dynamics of CO bound at the active site of myoglobin (Mb), a heme protein. In the last few years, weak tunable IR sources (especially diode lasers) have been successfully used to probe ligand photodissociation dynamics and rebinding kinetics of Mb-CO in flash photolysis experiments.[4,5] Instead of the more conventional uses of visible light to probe heme chromophores, a weak mid-IR source can be used to probe the vibrational absorption of the bound and free CO ligand. These flash photolysis experiments will not be discussed here. Instead, our intent is to describe another class of experiment, where an extremely intense mid-IR pump pulse is used to coherently drive the ligand's vibrational transition, and mid-IR probe pulses are used to investigate the dynamical interactions of these ligands at the active site of heme proteins with their surroundings. In particular, we will discuss the saturation recovery technique, often called a pump-probe experiment,[6-11] and the vibrational echo technique.[12-17]

New tunable coherent mid-IR ultrashort pulse sources fall into two general classes—tabletop laser systems with optical parametric amplifiers (OPA), and free-electron lasers (FEL). The work described here was performed using an FEL located at the Stanford FEL Center. The relative merits of OPAs and FELs have been discussed elsewhere.[18-20] It is worth mentioning that the cost of an OPA makes it an affordable possibility for an individual investigator research group, but mid-IR OPAs[21] are presently limited in power and in tuning range by the availability of very-high-damage-threshold nonlinear crystals which are transparent in the mid- and far-IR range. FELs are costly and ordinarily limited to large, multiuser facilities, but the ease of tuning and wide tuning range makes them an extremely versatile research tool. Furthermore, FELs are the only available source of readily tunable intense coherent pulses in the extremely important mid-IR 10–25-μm range, and the far-IR 25–100-μm range. Because FELs are perhaps less familiar to the biospectroscopy community than OPAs, and the use of FELs to study protein dynamics is quite new, we will devote some time in the next section to describe how FELs are used in this area. It is worthwhile to keep in mind that the experimental techniques we use at the Stanford Free-electron Laser Center do not intrinsically require an FEL. These powerful techniques can be used in individual investigator laboratories with tabletop OPA sources, provided the spectral transitions of interest lie within the tuning range of an available OPA.

Figure 1(a) shows the structure of Mb-CO, in the vicinity of the active site.[22] The carbonyl ligand is bound to the prosthetic group, protoheme, shown in Figure 1(b). Figure 1(c) shows the structure of a model heme compound discussed in later sections, M : coproporphyrin I, where M is a metal atom. Figure 2(a) shows the mid-IR spectrum of a concentrated $\sim$ 20 mM solution of Mb-CO in glycerol : water at 300 K. The $\lambda \sim 5.0$-μm carbonyl stretching fundamental is circled in the figure. The carbonyl stretch transition is the sharper peak on the larger broader background absorption. Figure 2(b) shows an expanded spectrum of the carbonyl stretch. Prior work has shown the existence of four distinct carbonyl stretching bands, which are assigned to four sets of protein conformers.[23,24] Conventionally these conformers are labeled A_0–A_3 in order of decreasing frequency. The most intense band in Figure 2(b) is the one denoted A_1, with a spectral width[25] of $\sim 10\ cm^{-1}$.

Conventional IR spectroscopy is not capable of revealing details of the fast dynamics of the bound ligand. Consider the problem of separating the carbonyl absorption and the broad background. The carbonyl transition is due to a lower concentration of an absorber with a large cross-section ($\sigma \sim 8 \times 10^{-17}\ cm^2$). The background arises from a much higher concentration of absorbers, e.g., water, glycerol, C–C stretches of the protein backbone, etc., with much smaller cross-sections. Conventional IR does not make a distinction between these different situations because it measures the sample absorbance, which is the product of the cross-section and the concentration.

In the pump-probe experiment, absorption saturation induced by an intense pump pulse is detected by a probe pulse. In the small-signal limit of an optically thin sample, the saturation level is linearly proportional to the cross-section, so the pump-probe signal is dominated by the carbonyl stretch.[18] Vibrational echoes are even more selective. In echo experiments,[26] an intense pulse creates a vibrational coherence. A second intense pulse rephases the coherence. When the coherence rephases, the sample emits a coherent echo pulse.[26,27] In the small-signal limit of an optically thin sample, the intensity of the echo signal is proportional to the fourth power of the cross-section. These are only two examples of techniques which make it possible to extract information from carbonyl vibrational transitions, in theory even if

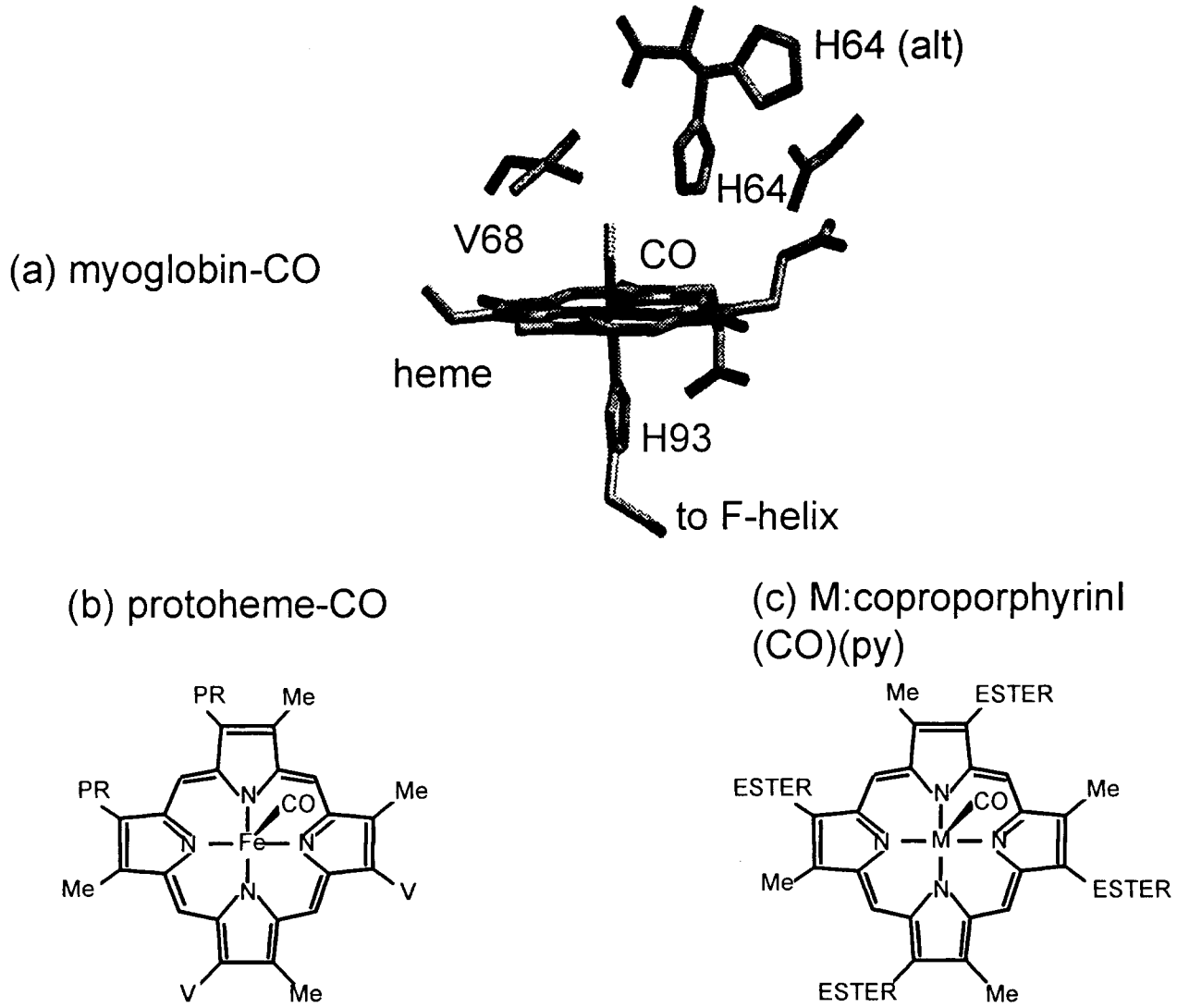

Figure 1. (a) Schematic diagram of the active site of wild-type myoglobin (WT Mb), adapted from Yang and Phillips.[22] H64(alt), the alternate position (the "up" position), is found to dominate at pH 4 and below. The down position for H64 is thought to be representative of the active site structure of the A_1 conformer and the up position of the A_0 conformer. (b) Structure of the prosthetic group in Mb, protoheme. (c) Structure of M : coproporphyrin I, where M is a metal atom. Key: Me = CH_3; V = CH = CH_2; PR = $CH_2CH_2CO_2H$; ESTER = $CH_2CH_2CO_2CH_3$.

these transitions were totally buried in a broad background of weak absorbers.

The vibrational lineshape of the carbonyl stretch is shown in Figure 2(b). The finite linewidth of the carbonyl stretching transition has been found to be due primarily to inhomogeneous broadening (see the final section in this article). Conventional IR spectroscopy of an inhomogeneously broadened spectrum provides no dynamic information whatsoever.[14,28] It provides only a measure of the static frequency spread of molecular oscillators.[29-31] Hidden beneath the inhomogeneous broadening is the homogeneous line. The width of the homogeneous line is due to fast dynamic interactions between the carbonyl oscillator and the protein.[30,32-34] These interactions cause the ensemble of carbonyl oscillators, which are driven coherently by mid-IR pulses, to undergo homogeneous dephasing, with a time constant T_2. The echo pulse sequence removes the effects of inhomogeneous broadening,[27] revealing the homogeneous lineshape, of width $\Delta\nu = 1/\pi T_2$. There are two distinct

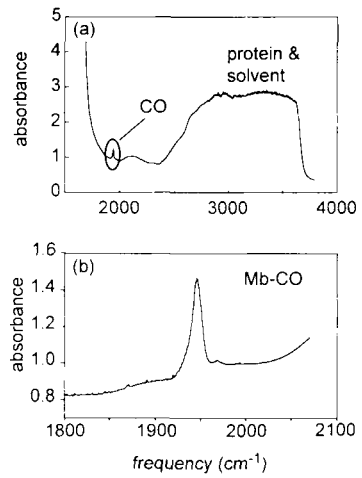

Figure 2. (a) Mid-IR spectrum of Mb-CO in glycerol: water. The circled region indicates the location of CO vibrational fundamental transitions on top of a broad background from protein and solvent. (b) Blowup of the CO stretching transition. Four distinct Mb-CO conformers, denoted A_0–A_3 in order of decreasing frequency,[23,24] have been found in this region. In this spectrum, the A_0 transition is seen as a small peak to higher frequency of the dominant transition A_1. The other two transitions are buried in the solvent background.

types of dephasing which cause homogeneous broadening. The loss of vibrational excitation from the excited carbonyl oscillator to the rest of the protein, with time constant T_1, is termed *vibrational energy relaxation* (hereafter VR). The loss of phase memory without loss of vibrational excitation, with time constant T_2^*, is termed *pure dephasing*. These three processes can be directly measured using pump-probe and echo spectroscopies.[32] Pump-probe experiments measure T_1. The echo measures T_2. The differences between the echo decay rate and the pump-probe decay rate can be used to determine T_2^*.

Studies of vibrationally excited CO have been used to investigate dynamics in many condensed phase systems, including CO dissolved in monatomic and diatomic liquids,[35,36] crystalline CO,[37] organometallic complexes in solution containing CO bound to a single metal atom or a cluster of metal atoms,[7,8,11,38] CO bound to clean metal surfaces,[39-41] CO bound to heme proteins,[4,5,42,43] and CO bound to model compounds.[42] Although the mechanical dynamics of such complicated systems are ordinarily quite difficult to treat theoretically, CO introduces several useful simplifications. CO is a computationally tractable diatomic molecule which binds to a variety of sites. CO vibrational relaxation can be investigated using the techniques of molecular dynamics,[44,45] because VR occurs on a suitable (subnanosecond) timescale. In contrast to simulations of picosecond time-scale photo-induced processes in Mb, such as photodissociation[46,47] or vibrational cooling,[48] carbonyl VR occurs solely on the ground electronic potential surface, and simulations need not invoke ad hoc assumptions about the nature of heme electronic transitions. The VR of excited CO can also be studied by exact quantum dynamic calculations, which are presently capable of modeling the short-time behavior of a diatomic molecule weakly coupled to a harmonic bath of arbitrary complexity. This possibility is especially intriguing in light of recent, highly accurate calculations of the vibrational density of states of a protein.[49]

An initial excitation of CO produced by mid-IR absorption will be localized on CO. Picosecond time-scale relaxation of CO vibrational excitation in heme systems occurs via weak anharmonic coupling to other vibrational states of the system,[50] resulting in a transfer of the CO vibrational energy to heme, the heme protein, and the solvent. Using the techniques of synthetic chemistry and site-directed mutagenesis,[51,52] it is possible to produce a wide variety of tailored Mb structures and analogs. Modified Mbs and models, combined with mid-IR dynamical measurements, for the first time open up the possibility of understanding the details of mechanical energy transfer at the active site of a protein and understanding how protein structure can influence molecular dynamics at the active site.

In the remainder of this article, we will describe the techniques for making these measurements using an FEL. Then we will present experimental pump-probe results obtained on wild-type proteins, mutant proteins, and heme model compounds, and echo data obtained on wild-type Mb. The quantum dynamical description of vibrational dynamics in condensed phases is discussed briefly, and a specific discussion of the relationships between heme structure and vibrational dynamics is considered. The mechanism of carbonyl VR is elucidated, and the dependence of VR rate on heme protein structure is discussed. Finally, a brief discussion of new approaches involving infrared vibrational echo spectroscopy is presented, and the complementary relationships between vibrational echo measurements and pump-probe measurements are discussed.

EXPERIMENTAL METHODS

Free-Electron Laser

A schematic diagram of an FEL driven by a linear accelerator (linac)[53] is shown in Figure 3. It is a

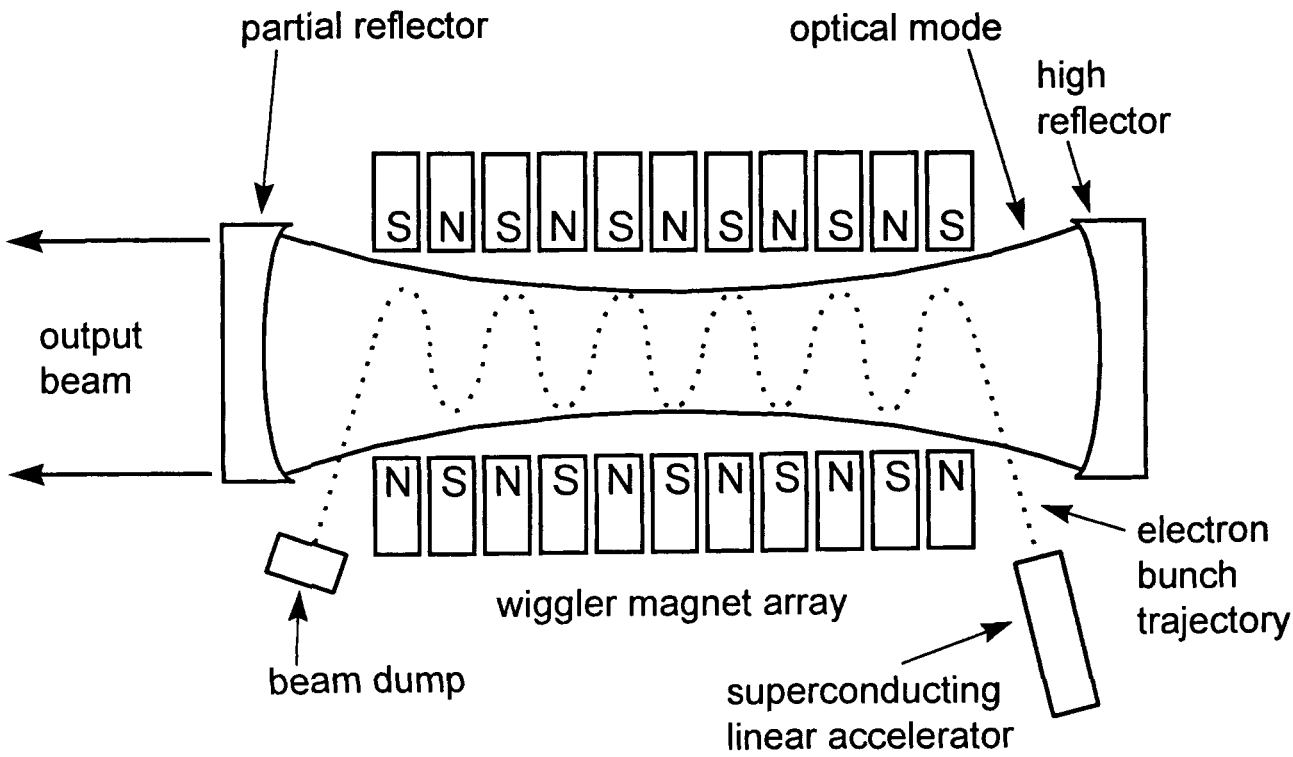

Figure 3. Schematic representation of a free-electron laser (FEL).

mode-locked laser, pumped by relativistic electron bunches. As the electrons propagate along the axis of a spatially periodic array of magnets, called a wiggler, they are accelerated transverse to their direction of motion, causing them to emit spontaneous radiation. This radiation is produced inside an optical resonator arranged so that it can interact with, and be amplified by, subsequent electron bunches. During operation of the FEL, the optical gain is larger than the losses, so the power in the resonator grows exponentially to saturation. The temporal characteristics of the train of optical pulses delivered by an FEL will match those of the generating electron beam.

The wavelength of the light generated by an FEL is determined by the energy of the electrons and by the parameters of the magnetic field. FELs do not, therefore, share the tunability limitations of conventional lasers. The accessible wavelengths are not determined by the properties of lasing media, but by attainable electron beam energies and magnetic field strengths. The wavelength can be controlled by adjusting either the electron beam energy or the magnetic field strength, and the optical pulse length can be varied by changing the electron bunch duration or by small changes in the optical cavity length to vary the degree of synchronization between the cavity round trip time and the electron bunch repetition rate. The FEL is thus an extremely flexible device.

There are two FELs at the Stanford Center,[54] both powered by the beam from a superconducting linac. These provide about 2000 h of FEL operation per year. The FEL used in heme protein work is designed to operate in the mid-IR, while the other (named FIREFLY) is designed for far-IR operation. Table I provides a summary of current operating parameters of the two FELs. Individual pulses of light are referred to as micropulses, while a train of micropulses is referred to as a macropulse. Since the linac delivers electron bunches at an 11.818-MHz rate, the separation between micropulses is 84.6 ns. The duration of each electron bunch is about 1 ps, but the optical micropulses can be adjusted to be somewhat shorter or longer than this value. When the micropulse duration is adjusted, the optical spectrum remains transform limited. Our experiments are typically performed using 1.5-ps pulses with spectral FWHM of 7.3 cm^{-1}. The Center is currently in the process of upgrading the linac. The result will be an increased energy in each micropulse by a factor of about 5 (to $\sim 5\ \mu J$), a greater range of micropulse durations, and an ability to extend the duration of mac-

Table I. Operating Parameters for the Free-Electron Lasers (FELs)

	Mid-Infrared FEL	Far-Infrared FEL (FIREFLY)
Wavelength	2–12 μm	15–100 μm
Micropulse duration	0.7–3 ps	2–10 ps
Micropulse repetition rate	11.818 MHz (84.6 ns)	11.818 MHz (84.6 ns)
Macropulse duration	5 ms	5 ms
Macropulse repetition rate	20 Hz	20 Hz
Micropulse energy	1 μJ	1 μJ
Average power	1.2 W	1.2 W
Spectral bandwidth	Transform-limited Gaussian	Transform-limited Gaussian
Spectral stability	0.01% rms	0.01% rms
Amplitude stability	< 2% rms	< 2% rms

ropulses to any desired value, or to provide a continuous stream of micropulses with no macropulse structure.

Two extremely useful features of this FEL are worthy of comment. Varying the duration of the transform-limited micropulses results in the ability to vary the spectral width. As the pulse duration is decreased, the optical spectrum becomes broadened, which has proven extremely useful in vibrational echo studies of vibrational anharmonicity.[13] Conversely, narrowing the spectrum can be desirable in studies of spectral diffusion. The relatively long spacing of ~ 85 ns between micropulses is an extremely useful feature of the Stanford FEL. It allows us to select single pulses or create pulse sequences using reliable acousto-optic modulators (AOMs).[55] Single-pulse selection is needed in pump-probe and vibrational echo experiments to avoid artifacts which always result from too-high pulse repetition frequencies.[56]

Figure 4 shows a representation of the layout of the Center, which is located in the W. W. Hansen Experimental Physics Laboratory. The linac and the FELs are located in a tunnel about 30 ft below ground level, to provide shielding from radiation produced by the high-energy electrons. The optical beams produced by the FELs are delivered via evacuated transport lines to the experimental laboratories in the first floor of the laboratory. About 10% of the beam is split off in the laboratory labeled FEL 1. The beam in FEL 1 is used for online diagnostics[57] and for feedback stabilization and control of the operating wavelength.[58] The diagnostics are ported to each of the laboratories to provide a continuous display of the spectrum, the pulse autocorrelation function and the beam power. The feedback-controlled wavelength stabilization system allows the operating wavelength to be selected and controlled by the experimenter. The heme protein experiments are performed in FEL 2. FEL 2 contains single-pulse selectors and a system which makes the invisible FEL beam collinear with a visible beam from a HeNe alignment laser. Three experimental stations in FEL 2 are set up to use the FEL beam: 1) a pump-probe and photon echo station; 2) a transient grating and stimulated echo station; and 3) a single-beam station. In FEL 3 and 4, facilities exist for two-color experiments,[59] which use FEL pulses and pulses from conventional laser systems. At the present time, a femtosecond Ti : sapphire laser, an amplified dye laser and a Nd : YAG laser are available in this facility.

Experimental Apparatus

Because of their inherent similarities, both pump-probe and vibrational echo experiments are performed using essentially the same experimental apparatus located in FEL 2. The design for this setup is diagrammed in Figure 5. In a pump-probe experiment, the sample is pumped by an intense pulse, and interrogated by a weaker probe pulse which travels down a variable optical delay line. In our experiments, the delay line can be scanned over a 1-ns range. The relative delay time between pulses is t_d, where $t_d = 0$ denotes the arrival time of the pump-pulse peak at the sample. The time-dependent absorbance change induced by the pump pulse, $\Delta A(t_d)$, is determined by measuring the intensity of the probe pulses transmitted through the sample. In our experiments the absorbance change is quite small, typically a few mOD units, so the probe-pulse intensity measurements must be very accurate. For this reason, we probe with two

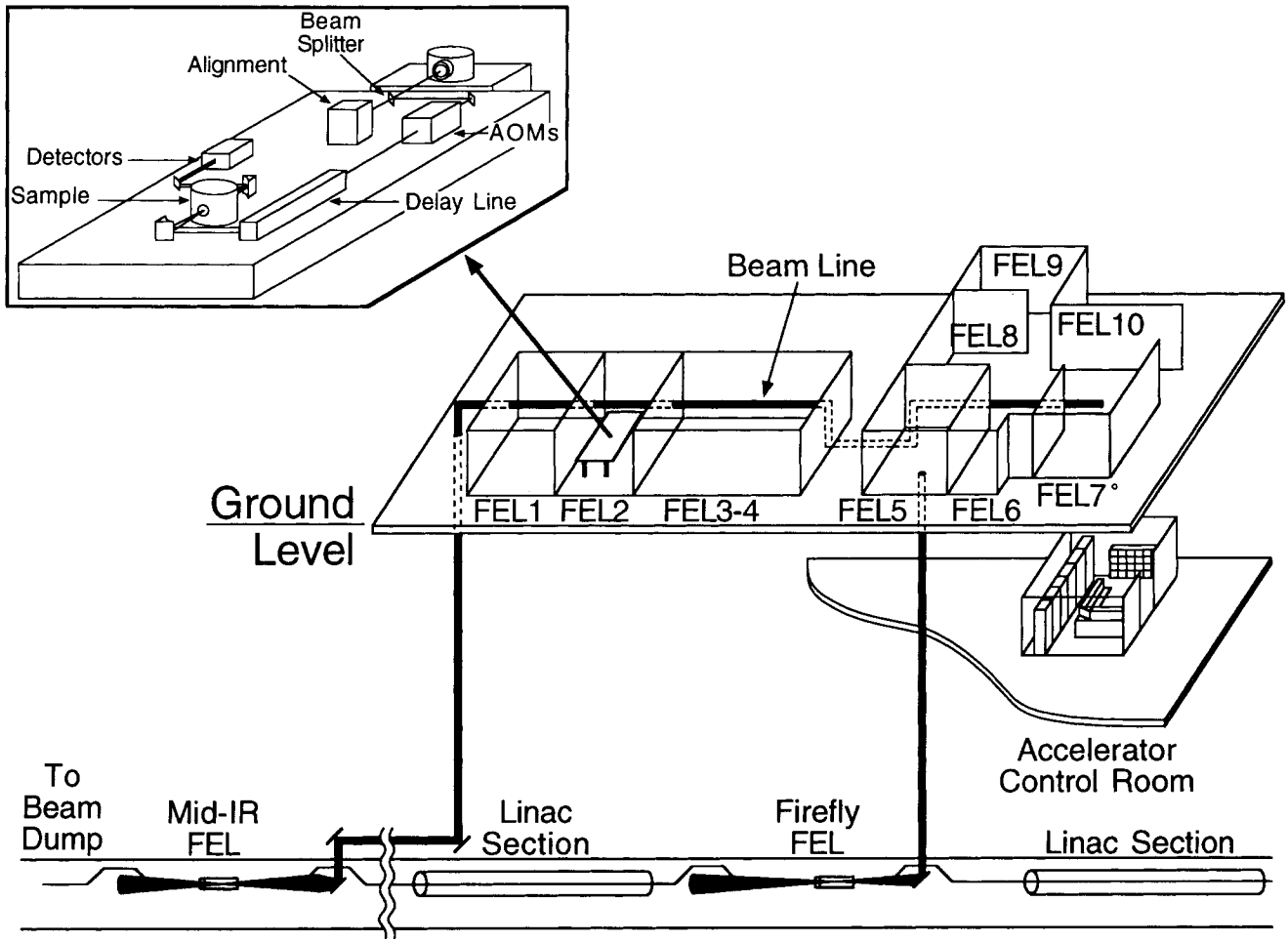

Figure 4. Schematic layout of the Stanford FEL Center, illustrating the superconducting linear accelerator (linac), the mid- and far-IR FELs, and the user experimental areas. FEL 1 contains diagnostic equipment. The heme experiments are performed in FEL 2.

adjacent[60] FEL micropulses. The first pulse of the pair arrives at the unperturbed sample ~ 85 ns before the pump. It is used as an intensity reference for the second pulse. The second pulse, which detects pump-induced absorbance changes, reaches the sample within 1 ns of the pump pulse arrival. Because of the relatively high Q of the FEL optical cavity, the two adjacent probe pulses are highly correlated in amplitude, wavelength, and temporal width. Determining $\Delta A(t_d)$ using two highly correlated adjacent probe pulses makes this detection scheme insensitive to laser fluctuations. Fast germanium AOMs are used to select appropriate micropulses from the FEL pulse train. At a 50-kHz repetition rate, the first AOM selects a pair of adjacent micropulses separated by 85 ns. The 50-kHz rate is determined by the limitations of the collection electronics, and it is low enough to avoid multiple pulse artifacts and significant sample heating. A 10% beamsplitter downstream of the first AOM is used to produce the probe beam. The bulk of the power is routed to a second AOM, where the second of the two pulses is selected to become the pump pulse. This pump pulse travels down a computer-controlled optical delay line before reaching the sample. Both pump and probe pulses are brought to a common focus 100 μm in diameter at the heme sample by an off-axis paraboloidal mirror. Typical pulse energies at the sample are 150 nJ for the pump pulse and 15 nJ for each probe. The samples are contained in a sealed optical cell with CaF_2 windows. For low-temperature work, this cell is mounted on the cold finger of a closed-cycle helium refrigerator or flow cryostat with a temperature range of 10–350 K. A second paraboloidal mirror is used to recollimate the beams. A fast infrared detector monitors the pair of probe pulses transmitted through the sample. Subsequent electronics

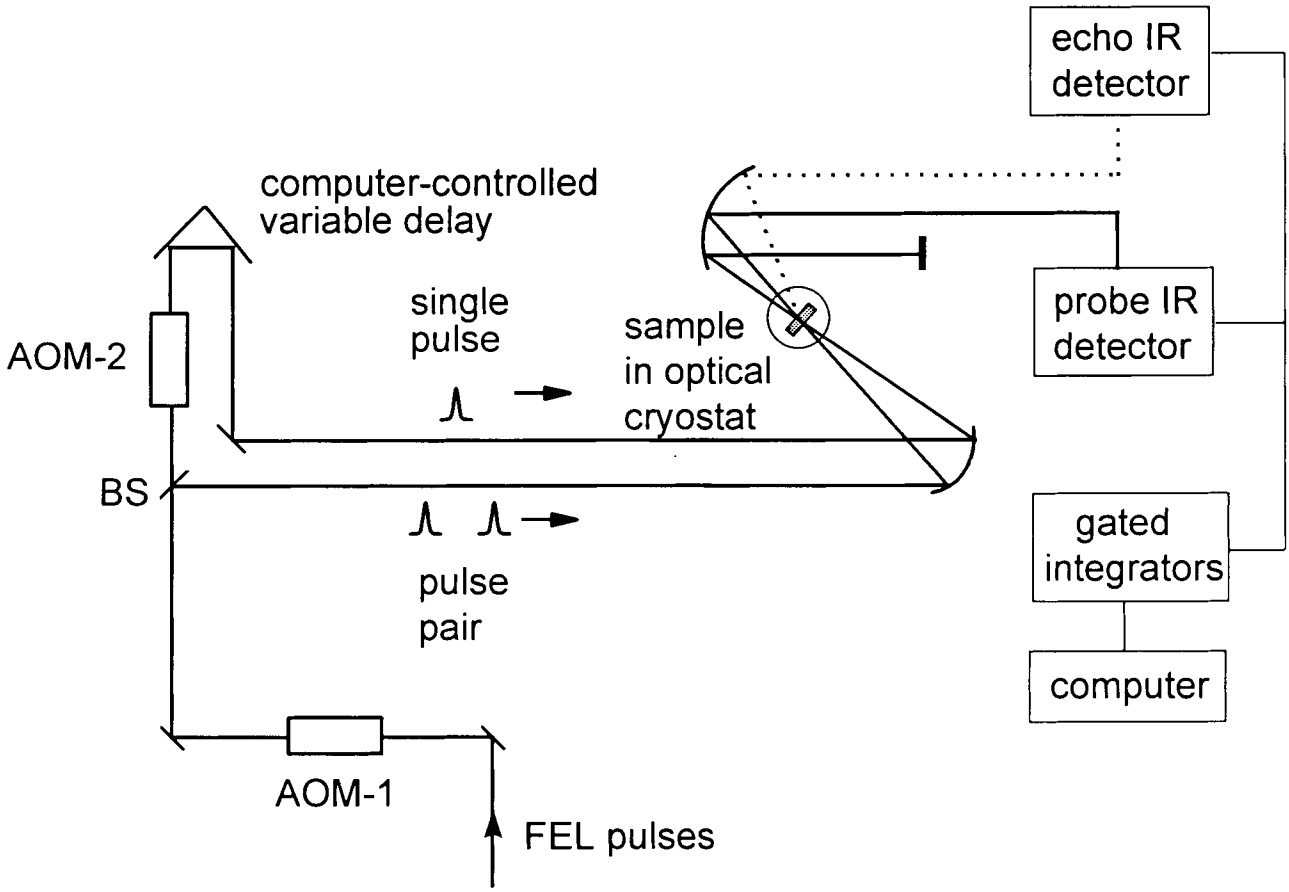

Figure 5. Schematic diagram of the apparatus used for pump-probe and vibrational echo measurements on Mb-CO. AOM denotes Ge acousto-optic modulators. The path of the echo signal emitted by the sample is indicated by the dotted line.

are used to integrate, subtract, and digitize the signal, which is then collected as a function of delay time t_d. Experiments can be performed with parallel pump and probe polarizations or with the probe at the magic angle. Careful intensity-dependent measurements are made to insure that the observed vibrational decay constants are not a function of the laser repetition rate or power, and that the sample remains chemically stable during data acquisition.

In echo experiments, the sample is irradiated by an intense pulse which coherently drives an ensemble of vibrational oscillators, which subsequently loses phase coherence. A second intense pulse, incident at time t_d, partially rephases the oscillators. When the partial rephasing is complete, a third pulse of light is emitted at time $2t_d$. This pulse, called the vibrational echo, is emitted by the sample in a unique direction and it can be separated spatially from the other pulses. Along with the echo signal, an unwanted optical background may also be detected owing to scatter of the intense pulses by the heme sample. The second rephasing pulse is predominantly responsible for this scattered light, since it is more intense and closer to the solid angle viewed by the echo detector. To reduce noise, it is advantageous to modulate the first driving pulse at half the frequency of the rephasing pulse (25 kHz).[11] The scattered light then occurs at a different frequency from the echo, and can thus be subtracted away. To switch from pump-probe to vibrational echo experiments, only minor modifications to the apparatus are needed. The AOM drivers are reconfigured to produce the echo modulation scheme, and the 10% beamsplitter used to produce the weak probe pulses is replaced by a 50% beamsplitter to generate the more intense second pulses needed in echo experiments.

Sample Preparation

Sample preparation has been discussed in detail in other publications.[42,60,61] The heme model com-

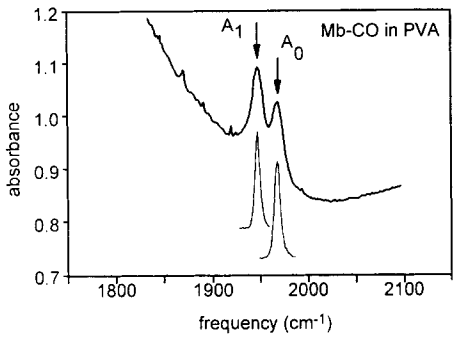

Figure 6. Mid-IR spectrum from Mb-CO in a solid matrix of poly-vinyl alcohol (PVA), reproduced from Hill et al.[61] In PVA, the relative intensity of the A_0 transition is enhanced, so both A_0 and A_1 protein conformers can be studied by pump-probe experiments. The lower curves indicate the spectra of FEL pulses used in these measurements.

pounds were synthesized in the laboratory of Professor Kenneth Suslick at the University of Illinois. The mutant proteins were synthesized in the laboratory of Professor Steven Boxer at Stanford University.

The signal-to-noise of the pump-probe and vibrational echo experiments is optimal when the absorbances of the carbonyl stretching transitions are in the 0.5–1.0 range, when the absorption background is minimized and when the sample does not scatter much of the pump and probe pulses into the detector. Absorption background is minimal in many of the solvents (e.g., CH_2Cl_2) used for the model compounds, but it is always a problem in the water–protein–glycerol samples. This background is minimized by using relatively high protein concentrations (typically 10–20 mM) and short optical path lengths (typically 0.4–0.8 mm). Light scattering is a particular problem when the proteins are embedded in solid matrices such as poly-vinyl alcohol, or low-temperature glycerol : water glasses. A certain patient artistry has been developed to maximize the heme concentration and minimize aggregation and glass-cracking effects which occur when the samples are cooled. In glycerol : water mixtures, adding more glycerol increases the quality of the glass at low temperature, but makes it more difficult to dissolve the protein. Much of the early pump-probe work was done with 75 : 25 glycerol : water solvent. More recently, we have begun to use 90 : 10 mixtures, which form excellent high-quality glasses needed for echo measurements. We have found that it is possible to produce a sufficiently high concentration protein solution ($\sim$ 15 mM) in this solvent mixture by very slow addition of protein with much stirring.

RESULTS OF PUMP-PROBE EXPERIMENTS

Myoglobin and Its Mutants at Ambient Temperature

The VR lifetime of the most intense carbonyl transition in Mb-CO [see Fig. 2(b)] in D_2O solution at ambient temperature, was reported by Hochstrasser and co-workers to be 18 ps.[4] The addition of glycerol to aqueous protein solutions is desirable for low-temperature studies, since glycerol is a cryoprotectant.[62] We have found the lifetime of Mb-CO to be essentially unaffected by glycerol.[61]

An extremely interesting result was obtained by studying Mb-CO in a solid matrix of poly-vinyl alcohol (PVA).[61] In PVA, the intensity of the A_0 conformer absorption is enhanced[24] and it becomes about equal to the absorption intensity of the A_1 conformer, as seen in Figure 6. Pump-probe experiments were performed on both A_1 and A_0 conformers,[61] located at frequencies 1946 and 1967 cm^{-1}, respectively. Figure 6 also shows the spectra of the 1.5-ps FEL pulses used to selectively pump each optical transition.[61] Figure 7 shows pump-

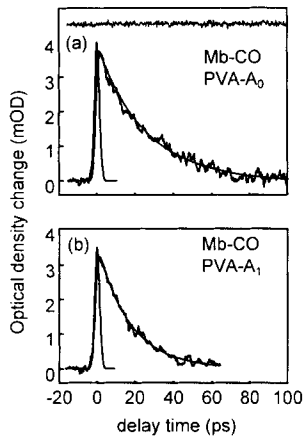

Figure 7. Pump-probe data on two conformers of Mb-CO in PVA at ambient temperature, reproduced from Hill et al.[61] The smooth curves are computed fits to exponential decays. Also shown are measured autocorrelation data on the 1.5-ps duration mid-IR pulses, representing the apparatus instantaneous time-response function. The horizontal trace at the top of (a) is a measure of the average intensity fluctuations of the probe pulses during the experiment. The different exponential decay constants of 26.6 (A_0) and 18.2 ps (A_1) demonstrate that different protein conformations can affect vibrational relaxation rates of ligands at the active site.

probe data on both conformers. The peak value of the induced absorbance change was a few mOD units. The horizontal data trace in Figure 7(a) is the output of the gated integrator which monitors the pump-probe intensity during the experiment. Over the ~ 30-min period of data acquisition, the extremely stable FEL pulses gave a noise level of a fraction of a mOD unit. Figure 7 also shows measurements of the pulse temporal autocorrelation function in a mid-IR autocorrelator,[19] which provides a direct measurement of the apparatus time response. The decays for both conformers are excellent fits to exponential functions (smooth curves in Fig. 7). The exponential decay constants, which give the VR lifetimes T_1 of these two states, are 26.6 ± 1 ps (A_0) and 18.2 ± 1 ps (A_1). Notice that the spectrum of the ~ 1-ps duration, transform-limited pulses in Figure 6 is narrow enough to resolve different Mb-CO conformers, while simultaneously the apparatus time response is fast enough to resolve the VR time constants. The ability to tune the FEL pulse duration, which simultaneously tunes the spectral width of the transform-limited pulses, is emerging as an extremely valuable attribute of this system. The exponential time constants, on the order of τ = 15–30 ps, correspond to frequency-domain Lorentzian linewidths $\Delta\nu$ = 0.1–0.3 cm^{-1}. Therefore, the contribution of VR to the much broader ~ 10-cm^{-1} vibrational line shapes seen in Figures 2 and 6 is negligible.[61]

Several different protein structures have been studied so far, as discussed in more detail in Hill et al.[60] For brevity, only a few of these will be discussed in detail. One important measurement involved the very interesting V68N mutant.[63] In this protein, valine-68 in the heme pocket [see Fig. 1(a)] is replaced by a more polar asparagine, resulting in a large carbonyl frequency redshift. Two bands at 1917 and 1933 cm^{-1} are observed, and at 300 K the 1917 cm^{-1} band studied here is dominant.[63] In Ref. 64, a comparison of the mid-IR and ^{1}H-NMR spectra of V68N and V68D was used to suggest that replacing V68 by V68N is accompanied by hydrogen bonding from asparagine to CO.[64] The VR lifetime of 10.5 ± 2 ps of this mutant[60] is considerably shorter than in wild-type (WT) Mb.

In the H93G(Im) protein, the proximal histidine H93 [see Fig. 1(a)] is replaced by glycine. Imidazole is added, which becomes bound to Fe and resides in a cavity in the proximal side of the protein.[65] In wild-type proteins, there is only one covalent bond path between CO and protein, which is the CO–Fe–imidazole–protein linkage. In the H93G(Im) structure, the imidazole–protein bond is broken. Despite cutting the only through σ-bond path from CO to protein, the VR rate of the A_1 state of H93G(Im) was identical to that measured for the A_1 state of WT.[60]

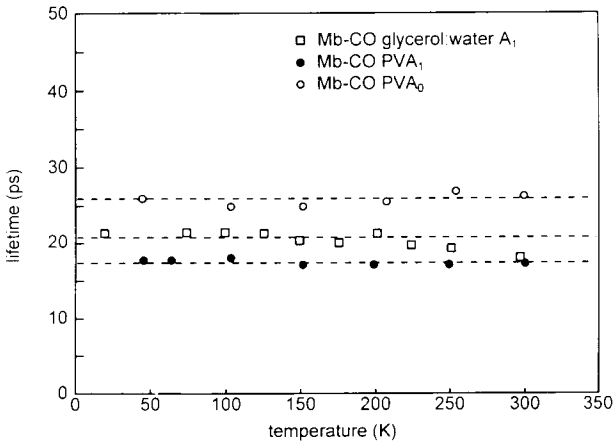

Figure 8. Temperature dependence of CO vibrational relaxation (VR) rates in myoglobin in glycerol : water or PVA. The dashed lines are visual guides. The A_1 state of Mb-CO in glycerol shows a small but detectable decrease in VR rate when temperature is lowered from 300 to 200 K. The VR rates in PVA do not change detectably with temperature. Reproduced from Hill et al.[61].

Myoglobin has several amino acids which are highly conserved in different species' proteins, but it is common for these proteins to otherwise differ at more than 20 amino acid residues.[66] In comparing wild-type proteins from human, sperm whale, and horse, and mutant human and sperm whale proteins,[60] a significant finding has emerged: Structural modifications to the protein, no matter how extensive, do not affect the VR rate if they do not affect the carbonyl-stretching frequency.

Temperature Dependence of Mb-CO Vibrational Relaxation

Pump-probe data were obtained on Mb-CO in glycerol : water and in PVA at different temperatures in the 20–300 K range.[61] The measured temperature-dependent T_1 decay times are plotted in Figure 8. The broken horizontal lines are visual guides. Within experimental error, no dependence of T_1 on temperature was observed for the PVA samples, which are solid throughout this temperature range. The A_1 state of Mb-CO in glycerol : water did evidence a very small temperature dependence. In cooling the sample from 300 to 200 K, which is approximately the glass transition[62] temperature, T_g,

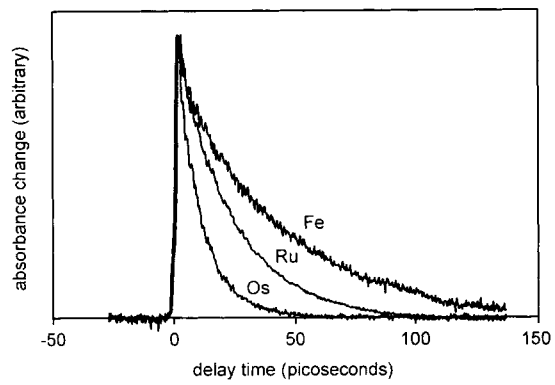

Figure 9. Picosecond mid-infrared pump-probe data on M(copro)(CO)(py) (M = Fe, Ru, Os) in CH_2Cl_2 solvent at ambient temperature. Reproduced from Hill et al.[42]

the lifetime increased slightly. Below T_g, we found T_1 was independent of temperature.

Heme Model Compounds

To better understand relationships between the active site structure and VR rates, we studied a number of model heme compounds.[42,67] In the model compounds we used, we have been able to study the effects of systematically varying porphyrin structure, the proximal ligand (proximal ligand denotes the ligand opposite CO), and the solvent. This work is discussed in more detail elsewhere.[42,67] Here we will primarily limit the discussion to an extremely interesting experiment where the mass of the metal atom was varied through the isoelectronic series, Fe, Ru, Os (mass 56, 101, and 190 amu).[42]

The compounds used were M-(coproporphyrinate I tetraisopropyl methyl ester) (CO) (pyridine); (M = Fe, Ru, Os); hereafter denoted M(copro)(CO)(py), dissolved in CH_2Cl_2. The pump-probe data on these three compounds are shown in Figure 9. The VR time constants were 42, 23, and 11 ps for Fe, Ru, and Os compounds, respectively. The heavier metal atoms resulted in faster CO VR rates.

Frequency Dependence of the Vibrational Relaxation Rate

In Figure 10 we plot VR rates versus the carbonyl stretching frequency ν_{CO} for the compounds discussed above. An important result shown in the figure is that for heme proteins and model compounds, the VR rates are correlated with ν_{CO}. The rates increase as the carbonyl stretching frequencies decrease. We wish to stress that many other mutant heme proteins and model compounds not shown[60] in Figure 10 evidence this same correlation.

The solid lines in Figure 10 are obtained by linear least-squares fitting of heme protein and model compound data, including protein data from other work[60] not displayed here. Over the frequency range accessible for these compounds, the functional form of VR rate versus frequency is consistent with a linear function, although other relationships which appear to be linear over this frequency range cannot be ruled out. The slope of the least-squares fit for the model compounds is quite similar to that seen in Mb and its mutants.[42] In fact, given the limited number of points, the slopes could be the same. Figure 10 also shows that at a given frequency, the VR rates in the model compounds are about 50% slower than in the heme proteins.

Figure 10 shows a quite small absolute change of frequency is associated with a large change in VR rate. Also in Figure 10, the absolute fractional change in carbonyl frequency is just a few percent, whereas the VR rates range over a factor of ~ 3.

Isotope Effects

Pump-probe experiments were performed on heme proteins[60] and model compounds[67] using ^{13}CO. One

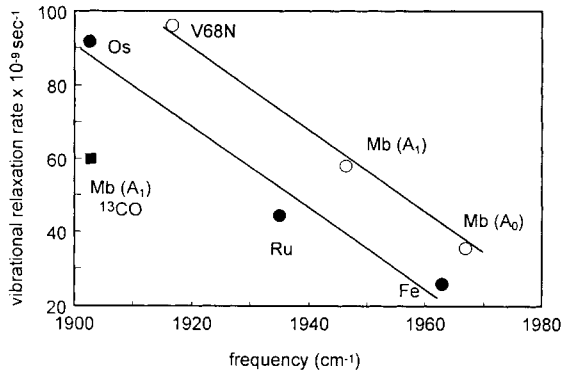

Figure 10. Plot of CO vibrational relaxation (VR) rate constants versus CO-stretching frequencies. For wild-type Mb and Mb mutants such as V68N (open circles), an apparent linear relationship is observed between the frequency and the VR rate constant.[60] Data for model compounds,[42] M-coproporphyrinate I tetraisopropyl methyl ester (CO) (pyridine) in CH_2Cl_2 solution (M = Fe, Ru, Os) are denoted by filled circles. The model compound data also show an apparent linear dependence with about the same slope as the Mb data. Replacing ^{12}CO with ^{13}CO in Mb-CO (filled square) causes a significant frequency redshift but does not change the VR rate of the A_1 conformer.[60]

result, shown in Figure 10, compares the A_1 state of ^{12}CO-Mb to the A_1 state of ^{13}CO-Mb.[60] There we see a relatively large frequency shift ($\sim 40\ cm^{-1}$), but the VR rate was unchanged by isotopic substitution. The same result was obtained using ^{13}CO with model compounds.[67] As in Mb-CO, the isotope frequency shift in model compounds was substantial, but the isotope effect on VR rate was negligible.

DISCUSSION OF PUMP-PROBE EXPERIMENTS

In this section, we first briefly describe the theory of infrared pump-probe experiments from a fundamental quantum mechanical point of view. Then we discuss these measurements from the point of view of molecular structure and protein dynamics. Following this general material, we will discuss the specific experimental results and what these results tell us about ligands at the active site.

Quantum Dynamic Description of Ultrafast IR Spectroscopy

The carbonyl stretching vibration is an anharmonic oscillator. In Mb-CO, the frequency of the fundamental $\mathbf{v} = 0$ to $\mathbf{v} = 1$ transition is $\sim 2000\ cm^{-1}$. Owrutsky et al.[4,5] used two-color mid-IR pump-probe experiments to show that the $\mathbf{v} = 1$ to $\mathbf{v} = 2$ transition is about $25\ cm^{-1}$ lower in energy than the $\mathbf{v} = 0$ to $\mathbf{v} = 1$ transition. The interpretation of our experiments is thus greatly simplified because the carbonyl oscillator can be treated as a two-level system. That approximate treatment is valid if the mid-IR pump pulses do not drive the carbonyl oscillator above the $\mathbf{v} = 1$ level. By carefully selecting and controlling the frequency of the IR pulse, the spectral width, and the intensity, we insure this will be the case.[13] The two-level system is weakly coupled to the surrounding medium (also termed the *bath*). The dynamical processes of interest here occur as a result of the weak coupling between the carbonyl oscillator and this medium.[50]

The dynamical behavior of the driven carbonyl oscillators can be described by a three-dimensional vector picture similar to one so successfully used to describe magnetic resonance experiments. A more detailed description of optical coherence experiments can be found elsewhere.[26] Here we will present just a simplified picture needed to interpret our results. The electric field E of a coherent transform-limited pulse at resonant frequency ω_0 is turned on for a time t_p. The electric field of the mid-IR pulses couples to the CO vibrations through transition matrix elements[28] of the form $\langle 1|\vec{\mu}\cdot\vec{E}|0\rangle$. By convention, the field E is taken to be aligned along the $+x$-axis of a Cartesian reference frame rotating at ω_0. A vector representing the ensemble-averaged dipole moment,[26] initially located along the $+z$-axis in the rotating frame, is caused to precess around x at an angular frequency $\omega_1 = \mu E/\hbar$. Once this vector is rotated from its equilibrium position along $+z$, it is perturbed by nonradiative relaxation processes. The radiative lifetime of carbonyl oscillators is typically a millisecond,[35] which is too slow to be significant in our experiments.

In both the pump-probe and vibrational echo experiments, the ensemble of carbonyl oscillators is driven by an intense first pulse. The probability of finding the system in the $\mathbf{v} = 1$ state increases with time during the pulse.[26] After a delay time t_d, during which the oscillators interact with the medium and undergo characteristic relaxation processes, a second pulse is turned on. The two experiments differ in the strength of the second pulse and the method of detection.

In the pump-probe experiment, the second pulse is a weak pulse and the intensity of this weak transmitted pulse is the quantity detected. This intensity is used to determine the instantaneous absorbance change at time t_d induced by the pump pulse, $\Delta A(t_d)$. The value of $\Delta A(t_d)$ is proportional to the instantaneous population difference between the ground and excited states. The time dependence of the pump-probe signal is given by[18]

$$\Delta A(t_d) = \Delta A_{max} \exp(-t_d/T_1), \qquad (1)$$

where ΔA_{max} is the peak absorbance change induced by the pump pulse, and time constant T_1 is the lifetime of excited $\mathbf{v} = 1$ carbonyl oscillators. The magnitude of ΔA_{max} increases linearly with pump-probe intensity and absorption cross-section in the small-signal limit.[18] As mentioned in the Introduction, this feature allows pump-probe measurements on the carbonyl stretching transition to discriminate against the large background seen in Figures 2 and 6 consisting of absorbers with small cross-sections.

In the echo experiment, after the vector is rotated from its equilibrium position, the individual oscillators begin to dephase at a rate $\sim 1/\Delta\nu$, where $\Delta\nu$ represents the frequency spread of oscillators driven by the coherent pulse.[26] When the coherent pulse duration t_p is shorter than the dephasing rate, $\Delta\nu$ is the width of the spectral transition.

It is the usual practice to describing dephasing as arising from three distinct sources.[30,32] Inhomogeneous dephasing results from "slow" interactions between the oscillators and the medium, where the meaning of slow is discussed below and in more detail elsewhere.[32] The slow interactions induce a spread of oscillator frequencies (inhomogeneous broadening) which does not change during the echo time scale. The echo time scale is on the order of a few multiples[32] of T_2. Homogeneous dephasing results from two fast processes which affect any oscillator. The T_1 or lifetime process causes dephasing due to nonradiative transitions from $\mathbf{v} = 1$ to $\mathbf{v} = 0$. The pure dephasing process involves phase-changing interactions which do not affect the population. Pure dephasing is characterized by the time constant T_2^*. The relationships between these parameters can be summarized by the equations[26,32]

$$(\Delta\nu)^{-1} \leq T_2 \leq 2T_1, 0 < T_2^* < \infty, \qquad (2)$$

and

$$1/T_2 = 1/T_2^* + 1/2T_1. \qquad (3)$$

In proteins, glasses, and other disordered media, the structure of the medium is not static. Instead, the structure evolves in time, and ordinarily the dynamics of structural evolution occur over a wide range of time scales. When significant structural evolution occurs on the time scale of T_1 or T_2^*, the conventional treatment[30] of dephasing is no longer adequate. The reader is referred to Berg et al.[32] and Bai and Fayer,[33] where the precise meaning of these time constants needed to interpret optical coherence experiments in proteins is discussed in detail.

Quantum Dynamic Description of Relaxation Processes

Vibrational relaxation and vibrational dephasing occur through the interaction of the system with other vibrational degrees of freedom of the medium. In theoretical treatments of vibrational dynamics, this interaction is described by a force correlation function.[50,68] The force correlation function has been treated classically[68] and more recently, quantum mechanically.[50] In addition to the laser-excited carbonyl oscillators at frequencies near ω_0, at finite temperature a vast number of modes of the medium are excited. The excited modes produce a broad spectrum of structural fluctuations. Some or all of the fluctuating modes that are coupled to the system exert forces on it. These forces are described by the force correlation function. The pure dephasing and VR are driven by higher-frequency Fourier components of the force correlation function. These are the "fast" interactions mentioned above. The VR is driven solely by the Fourier component at ω_0, whereas the pure dephasing can be driven by a broader range of lower frequencies.[32,50] The low-frequency or zero-frequency Fourier components of the force correlation function cause inhomogeneous dephasing. These are the "slow" interactions mentioned above. The effects of these slow interactions can be removed by the echo pulse sequence.

In the classical mechanical description of the force correlation function, only thermally excited modes contribute to T_1. The VR rate depends on the occupation numbers, n, of the modes of the medium that contribute to the Fourier component of the force correlation function at ω_0. The occupation numbers are temperature dependent and for a mode of fundamental frequency ω; they are given by the Bose–Einstein function

$$n_\omega(T) = [1 - \exp(\hbar\omega/kT)]^{-1}. \qquad (4)$$

In the quantum mechanical description of the force correlation function,[50] an important new feature emerges. It is found that the rate of T_1 relaxation depends on $(n + 1)$ rather than n. The quantum mechanical description of T_1 is analogous to the more familiar problem of a radiative transition being driven by a radiation field. The T_1 process, owing to its $(n + 1)$ dependence, has a finite rate even at zero temperature.[50] The zero-temperature VR process occurs when the driven oscillator decays by exciting modes of the medium. This is analogous to spontaneous emission in a radiative system, where radiative relaxation can occur even in the absence of a radiation field to stimulate emission.[26] As temperature is increased, and modes of the medium become thermally excited, the rate of VR increases. This increase is analogous to stimulated emission in a radiative system. In this discussion, we emphasize the results of the full quantum mechanical treatment because the classical mechanical model cannot explain the temperature dependence of our VR data.[60]

Molecular Mechanical Treatment of Vibrational Relaxation

We now discuss VR of the carbonyl stretch, taking into account details of the highly structured me-

dium consisting of heme, protein, and solvent. VR occurs by anharmonic coupling between the excited carbonyl and states of the medium at the high frequency ω_0 (ω_0 is in the mid-IR range). Speaking qualitatively and classically, anharmonic coupling means that displacements of the carbonyl oscillator can induce displacements of other atoms of the medium.[60] This medium has a vast number of states at ω_0, so VR is an irreversible process.

The normal modes of the medium consist of heme vibrations, protein vibrations, and solvent vibrations.[61] Here we use the term *vibration* to indicate intramolecular normal modes which principally involve displacements from equilibrium of covalently bonded atoms. In addition, the protein[34,49] and solvent[35] each have a lower-frequency continuum of modes which range from zero frequency to a cutoff lying in the few hundred cm^{-1} range. These continuua are analogous to the phonon modes[31] of a crystalline solid. In the subsequent discussion we will simply use the term *phonons*. However, the phonon description is only precise for ordered media with well-defined structure, whereas protein and solvent are disordered media with continually evolving structures. The term *instantaneous normal intermolecular modes* is a more precise description of these states.[69-71]

Owing to the unusually strong C–O bond in metal carbonyls, there are essentially no fundamental modes of the medium resonant with the carbonyl stretch. However, there are a vast number of states resonant with this excitation. These states consist of combinations and overtones of the normal modes of the medium. For just one of many possible examples, a combination of two C–C stretching modes ($\sim$ 1000 cm^{-1}) plus one phonon (0–100 cm^{-1}) might be resonant with the carbonyl fundamental. The density of these combination and overtone states increases rapidly with increasing energy. Combinatorial mathematics shows the density of states increases approximately exponentially with increasing energy.

In the force correlation function description of carbonyl VR,[50] we are not concerned with all the states of the medium, just states which couple efficiently to the carbonyl stretch. The molecular mechanical description provides insight into these couplings. Vibrational energy transfer is ordinarily thought to be more efficient when strong covalent bonds are involved, as opposed to weaker nonbonded interactions.[50] However, Figure 1 shows that there is only a single covalent bond between CO and heme. CO also interacts with the porphyrin macrocycle via π-bonded interactions, and it interacts with protein via a large number of weak nonbonded, and perhaps in some structures hydrogen-bonded, interactions. It is not immediately obvious which of these interactions would be dominant, or whether all might contribute significantly to the VR process. Now we will consider the mechanics of anharmonically coupling CO vibrations to protoheme, to amino acids in the distal heme pocket, and to the proximal side of the protein.[60]

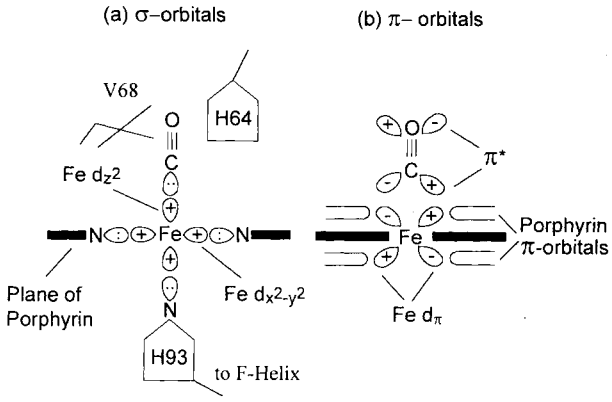

Figure 11. Schematic diagram of some of the orbitals involved in CO binding to heme. (a) The through σ-bond anharmonic coupling model for vibrational relaxation involves displacements of CO which couple directly to motions of Fe. (b) In through π-bond anharmonic coupling, the π^*-orbitals of CO interact with the π-orbitals of the metalloporphyrin ligand, which produces anharmonic coupling between the CO stretch and porphyrin ring vibrations. Different protein structures, e.g., V68 mutants, can shift the carbonyl frequency by changing the extent of back-bonding. The rate of vibrational relaxation via through π-bond coupling increases with increasing back-donation from porphyrin to the π^* orbitals of CO. Reproduced from Hill et al.[60]

Figure 11 is a schematic diagram of the carbonyl binding site in Mb, showing some of the σ- and π-orbitals involved in covalent protoheme–CO bonding.[60] The expected geometry of Fe–C–O in heme systems is a linear complex oriented perpendicular to the heme plane, based on orbital overlap in the π-back-bonding model of transition metal carbonyl complexes.[72] Many experiments have suggested it is difficult for a protein to tilt CO significantly.[73,74] This view is reinforced by recent IR dichroism work[75] and polarized IR measurements of oriented wild-type Mb single crystals.[76]

Through σ-bond coupling is the term we use for vibrational energy transfer processes from CO to heme,[42] involving the strong σ-bond between Fe and C [Fig. 11(a)]. The through σ-bond mechanism implies a coupling between the carbonyl

stretch and porphyrin modes which involve displacements of Fe, such as Fe–CO stretching or bending. A similar scheme used to model the VR of a diatomic A–B molecule bound to a third atom M, coupled to a bath, has been discussed by Benjamin and Reinhardt.[77] Both classical and quantum mechanics predict that through σ-bond coupling will be reduced by substituting heavier isoelectronic metal atoms for Fe. Viewed classically, carbonyl-stretch–induced metal atom displacements will be smaller with heavier metal atoms, resulting in slower damping of the CO oscillator. Viewed from the force correlation function description, lower frequencies of the modes associated with the heavier metal atoms will result in smaller Fourier coefficients of the force correlation function at the CO transition frequency ω_0.

Through π-bond coupling is the term we use for vibrational energy transfer processes from CO to protoheme involving the extensive delocalized π-bond network shown[42] in Figure 11(b). Formation of a σ-bond between Fe and CO is accompanied by back-donation from the heme π-orbitals (the combined metal d_π (d_{xz} and d_{yz})/macrocycle p_π orbitals) to the carbonyl π^* antibonding orbitals.[77] The extent of backbonding can be influenced by the structure. When the extent of back-bonding is increased, the CO bond weakens, the equilibrium CO bond distance lengthens, and the CO vibrational frequency decreases. Simultaneously the Fe–C bond strengthens, the equilibrium Fe–C bond shortens, and the Fe–C vibrational frequency increases.[73,79]

Structural fluctuations of the macrocycle or its surroundings (protein or solvent) produce fluctuations of the π-electron cloud, which modulate the back-bonding to CO. Changes in back-bonding change the vibrational potential. Since force is the derivative of the potential, structural fluctuations of the macrocycle produce fluctuating forces on the CO oscillator.[50] In the context of the classical force correlation function description, the fluctuations are caused by the thermally populated modes of the macrocycle, and the Fourier component at the CO transition frequency ω_0 drives the relaxation. The quantum mechanical treatment shows that it is not necessary for these modes to be populated, because carbonyl VR into macrocycle vibrations can occur through spontaneous emission.[50] While not identical to the problem under consideration here, a detailed orbital description of the coupling between a vibrationally excited CO bound to a metallic surface, interacting with labile electrons of the metal, has been presented by Head-Gordon and Tully.[45]

Vibrational energy transfer from CO to the distal heme pocket would involve coupling through nonbonded interactions between CO and distal amino acid residues, most likely H64 and V68 (see Fig. 1). In some heme conformations, and in some of the mutants we have studied, there is the possibility for specific chemical interactions with CO such as hydrogen bonding between distal amino acid residues, CO, and water molecules in the heme pocket.[60,72] Coupling through hydrogen bonds might be expected to be more efficient than coupling through nonbonded interactions, but in the heme pocket there are many nonbonded interactions and few or perhaps no hydrogen bonds. The relative significance of these different types of coupling cannot be determined a priori. Vibrational energy transfer from CO to the proximal side of the protein could occur by through σ-bond coupling. As shown in Figure 11(a), displacements of CO could induce displacements of Fe and the proximal histidine H93, which could be transmitted to the F-helix of the protein.

Temperature Dependence of Vibrational Relaxation

Figure 8 shows that the vibrational lifetime of CO bound to Mb is essentially temperature independent between room temperature and 10 K.[61] At room temperature, $kT \approx 200$ cm^{-1}. Therefore, at room temperature, lower-frequency modes < 200 cm^{-1} will have significant occupation numbers and much higher-frequency modes will have negligible occupation numbers. In the 10–300 K range, only the occupation numbers of the lower-frequency modes change significantly. If these lower-frequency modes were involved in CO vibrational relaxation, a substantial increase in the vibrational lifetime would result by decreasing temperature from 300 to 10 K. The lack of a temperature dependence in this range demonstrates that only higher frequency modes are involved in the vibrational relaxation. Analysis of temperature-dependent data showed these higher-frequency modes must lie in the > 400-cm^{-1} range.[42] In classical mechanics these > 400-cm^{-1} modes, which are not significantly populated at the temperatures of interest, would play virtually no role in VR. In the quantum mechanical treatment of VR, even the higher-frequency modes contribute to the forces felt by the excited carbonyl oscillator owing to their zero-point energies. The predominant mechanism of carbonyl VR is analogous to spontaneous emission

of these higher-frequency excitations, which is a purely quantum mechanical process.

Isotope Effects and Induced Shifts

Figure 10 shows that when different protein structures or different model compounds are used, the VR rate increases in a roughly linear fashion as the carbonyl frequency decreases. But when ^{13}CO is used, the carbonyl frequency decreases substantially while the VR rate remains unchanged. The magnitude of the force correlation function at the carbonyl oscillator frequency depends on the density of states at this frequency, and the coupling strength between the oscillator and the medium. The effects of changing the structure might be manifested by changes in the density of states, the coupling, or both.

The ^{13}CO results allows us to rule out the possibility that the VR rate depends explicitly on the absolute value of the frequency.[60] Such a dependence might exist, for example, if the density of states for the VR process varied significantly over the $\sim$ 1900–1980-cm^{-1} range of carbonyl stretching frequencies. If a frequency shift simply moved the vibrational frequency to points of higher or lower density of states, thereby causing a change in the VR rate, then the shift caused by the ^{13}C substitution would also change the VR rate, which it does not. Therefore, protein-induced effects on the VR rate must be due to a change induced by the protein matrix in the coupling of the CO vibrational excitation to the rest of the heme-protein system.

Through π-Bond Coupling Is Dominant

In the model compounds, VR might involve: 1) through σ-bond coupling from CO to heme; 2) nonbonded interactions between CO and solvent (here CH_2Cl_2); or 3) through π-bond coupling to heme.[67] Through σ-bond coupling is immediately ruled out, because the results in Figure 10 are exactly opposite those expected for this mechanism.[42] The heavier metal atoms would greatly decrease the rate of VR owing to through σ-bond coupling. Nonbonded interactions were investigated in experiments where the VR of Ru(Copro)(CO)(Pyr) was studied in different solvents.[67] We found the VR rate hardly changed when CH_2Cl_2 was replaced by other chlorinated hydrocarbons such as CH_3CCl_3 and CCl_4. Changing these solvents has a substantial effect on the density of states of the surrounding solvent, and therefore, these results rule out a significant contribution from vibrational energy transfer via nonbonded interactions with the solvent. (They do not rule out the possibility of energy transfer from CO to other strongly complexing or hydrogen-bonding solvents.) Thus, VR in the model compounds ought, by elimination, to be dominated by through π-bond coupling.

The strongest affirmative evidence for through π-bond coupling in model compounds is the inverse relation between carbonyl frequency and VR rate.[42] The polarizability of the d^6 electrons increases in the order Fe, Ru, Os; so the extent of backbonding from the metals' d^6-electrons to CO increases in the same order.[78] Thus, the VR rate increases with the extent of back-bonding in the model compounds. Increasing back-bonding is associated with carbonyl frequency lowering. Thus, the through π-bond model explains how decreasing the carbonyl stretching frequency can result in an increase in the VR rate.

Based on the model compound results, and the strong similarity between the protein data and the model compound data in Figure 10, we can conclude that VR in Mb-CO must involve, at a minimum, a significant contribution from through π-bond coupling from CO to heme. There is no reason to believe that through σ-bond coupling from CO to heme is any more efficient in Mb-CO than in the model compounds. The H93G(Im) experiment allows us to rule out the possibility of through σ-bond coupling between CO and the protein, because cutting the covalent σ-bond linkage between heme and protein did not affect the VR rate at all. One other possibility worth considering involves anharmonic coupling between CO and amino acids in the distal protein pocket through nonbonded interactions, or hydrogen-bonded interactions in structures where H-bonds are present.

The role of interactions between CO and the surrounding protein can be investigated using proteins with different structures. Changing the protein structure may change the through π-bond coupling between CO and heme, and also open up channels for energy transfer from CO to protein. It is difficult to separate these two protein effects cleanly. As discussed subsequently, we believe at least some of the difference in absolute VR rates between Mb and model compounds seen in Figure 10 (i.e., proteins and model compounds with the same ν_{CO} have different VR rates) is due to the difference between CO–protein interactions and CO–CH_2Cl_2 interactions. To date, no convincing evidence has been found to indicate that different proteins open up different specific channels for VR,

because in all our experiments, the VR rates in different myoglobins appears to depend primarily on the induced carbonyl frequency shift, and not on the details of how the shift is induced by the protein matrix.[60]

Vibrational Relaxation and Protein Conformers

The Mb-CO mid-IR spectrum provides evidence for different protein conformers. The carbonyl stretching transitions A_0–A_3 indicate the coexistence of at least four primary conformers.[23] The line shapes of the A-bands evidence Gaussian components which are frequently indicative of inhomogeneous broadening.[24] The existence of a secondary set of conformers within each A-state (termed a second *tier of substrates*) was proposed by Frauenfelder and co-workers[80,81] to explain the nonexponential time dependence of CO rebinding seen in flash photolysis experiments,[24] where mid-IR light was used to selectively probe the different A-bands.[24] Our echo data in the 80–300 K range provide convincing proof that the A_1 transition is inhomogeneously broadened. Therefore, we have proven that distinguishable conformational states exist within an A-band, which are characterized by slightly different carbonyl transition frequencies, which cannot interconvert on the time scale of the echo experiments, even at ambient temperature.

The VR rates of different A-states (i.e., A_0 and A_1) are clearly different. However, when we perform a pump-probe experiment on an A-state, we observe an exponential decay (Fig. 7), proving that all the proteins excited by the laser pulse (as shown in Fig. 6, our laser pulse spectrum is somewhat narrower than the A-state spectrum) have indistinguishable VR kinetics.[61] This observation shows that VR rates are not affected by protein conformational changes which do not significantly affect the carbonyl-stretching frequency.[61]

Vibrational Relaxation and Heme Protein Structure

In our studies of mutant and WT heme proteins, we have investigated the effects of many different structural changes,[60,61] although, of course, we have not exhausted even a tiny fraction of all possibilities. Our general conclusion based on the structures studied to date is that structural modifications, no matter how extensive, do not affect the VR rate unless they also affect the carbonyl-stretching frequency ν_{CO}. For example, we compared H64V mutants, where distal histidine is replaced by valine from both human and sperm whale. These structures differ at more than 20 amino acid sites, but they have the same ν_{CO} and identical VR rates.[60] In comparing H64V to H64L mutants (in H64L, H64 is replaced by leucine), it has been found that the CO-binding affinity in H64L is much larger than in H64V.[72] This affinity difference has been attributed to stabilization of CO by leucine. Even though the interactions between protein and CO are evidently somewhat different in these two mutants, these different interactions do not have a significant effect on ν_{CO}. Both mutants have the same ν_{CO} and the VR rates are virtually identical.

In the V68N mutant, ^{1}H-NMR and low-temperature mid-IR measurements[64] show there is a hydrogen bond between asparagine and CO which does not exist in WT proteins. The hydrogen bond increases the back-bonding from CO to heme. The increase in the VR rate caused by increasing the through π-bond coupling is consistent with the linear relationship observed in all the other proteins studied. The hydrogen bond might provide a direct channel for vibrational energy transfer from CO to asparagine, but if this effect exists at all, it must be smaller than the CO to heme relaxation channel.[60]

If the details of protein structure had an effect on the VR rate other than the total resultant influence on back-bonding, one might expect a rather complicated dependence of VR on structure and vibrational frequency. However, such a complicated relationship is not consistent with the simple linear dependence seen in the data. These results imply that the dominant influence of protein modifications on VR is to change the back-bonding from the heme to the CO.[60]

How Myoglobin Affects Vibrational Relaxation at the Active Site

We earlier listed two possible ways the protein could affect VR at the active site. We now may conclude that the protein influences molecular dynamics of bound ligands at the active site primarily via a passive mechanism where the protein electric field alters the through π-bond coupling between CO and heme, rather than an active mechanism in which different protein structures open up new channels for energy transfer from the ligand to the protein.[60]

Vibrational Relaxation in Proteins Versus Model Compounds

Figure 10 shows that the absolute values of the frequency-dependent VR rates are about 50% slower

in the model compounds than in the mutant proteins. We have conducted experiments[67] with the intent of better understanding the relationships between these differing molecular structures and the VR rates. In Mb the proximal ligand is imidazole, and in the model compounds it is pyridine. We have studied model compounds that are otherwise similar, but which are bound to many different proximal ligands.[67] Although some proximal ligands can affect the VR rate, substituting imidazole for pyridine had essentially no effect on VR. The structure of protoheme found in Mb differs slightly from coproporphyrin I (cf. Fig. 1), but experiments on different porphyrin modifications again show this difference to be small. More substantial structural changes, however—for example, substituting sulfonated phenyl groups on the porphyrin perimeter[42]—can have a consequential effect. The VR rates and carbonyl frequencies in the model compounds do depend somewhat on solvent. It takes a rather substantial change in solvent properties to induce an ~ 50% change in VR rate, e.g., changing CCl_4 to an aromatic solvent such as dibutyl pthalate. In the model compounds, coproporphyrin is dissolved in CH_2Cl_2. In Mb, heme is embedded in a protein. This is a sufficiently drastic change in solvent (protein environment vs. CH_2Cl_2) to be capable of inducing a 50% change in VR rate. Thus, we attribute the differences in absolute VR rates between the model compounds and the proteins to differing local solvent environments, but understanding the details of how different solvent environments influence the VR rate requires further study, as discussed in more detail elsewhere.[67]

A NEW APPROACH: IR VIBRATIONAL ECHO EXPERIMENTS

Echoes and Pure Dephasing

Like the pump-probe experiments, in vibrational echo experiments a first pulse is applied which coherently drives the carbonyl oscillators. However, in the echo experiment the second pulse at time t_d is not a weak probe, but it intentionally perturbs the driven oscillators. The second pulse is intended to reverse the trajectories of the oscillators driven by the first pulse,[26] in a manner analogous to the spin-echo technique. The trajectories would be perfectly reversed, and the dipoles would rephase at time $2t_d$, provided the individual oscillator frequencies remained constant on the echo time scale.[32,33] This is the case for oscillators which are perturbed solely by the slow interactions which are responsible for inhomogeneous broadening of the vibrational transition. The rephased dipoles will emit a coherent pulse of mid-IR light, the vibrational echo. Because the thickness of the sample (~ 400 μm) is much greater than the ~ 5 μm wavelength of mid-IR light, the echo is emitted primarily in the phase-matched direction,[27] as shown in Figure 5. Any dipole which was perturbed by fast interactions will not be perfectly rephased by the second pulse. As time t_d is increased, the fraction of dipoles which are dephased by fast interactions increases. The amplitude of the collective dipole which produces the echo declines. The echo decay is given by[32]

$$I_{echo}(t_d) = I_{echo}(0)\exp(-4t_d/T_2)$$
$$= I_{echo}(0)\exp[-4t_d/(2T_1 + T_2^*)]. \quad (5)$$

The factor of four in the numerator of the exponentials in equation 4 arises because the echo is emitted at time $2t_d$, and its intensity is proportional to the square of the collective dipole moment.[26,27] In our experiments, the value of $I_{echo}(t_d)$ depends on the pulse intensity to the third power and the absorption cross-section to the fourth power. The echo experiment discriminates between the intense carbonyl transition and the background absorption to even a greater extent than the pump-probe experiment.

In the force correlation function treatment of pure dephasing, pure dephasing is seen to differ from VR in two significant ways. The rate of pure dephasing depends on the occupation numbers n of the medium, rather than $(n + 1)$, so only thermally excited modes of the medium contribute to pure dephasing.[32] The rate of pure dephasing goes to zero at zero temperature ($T_2^* \rightarrow \infty$ as $T \rightarrow 0$). VR is induced only by Fourier components of the medium[50] at frequency ω_0, whereas pure dephasing can be induced by a broader spectrum of medium fluctuations.[32] Thus, vibrational echo studies of pure dephasing can be used to investigate protein dynamics on a broader range of time scales than VR studies, and in particular permit investigation of some of the slower conformational relaxation processes which would have no effect on VR.

Vibrational Echo Experiments

We have recently performed the first successful vibrational echo experiment on a vibrational transi-

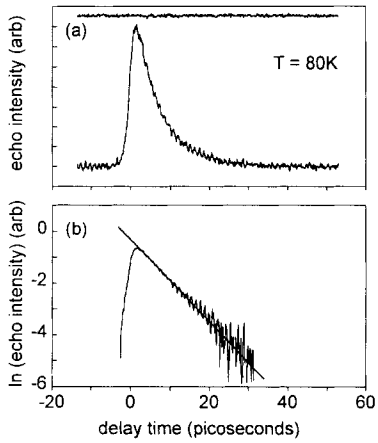

Figure 12. Vibrational echo data on Mb-CO (A_1 conformer) in glycerol : water, at 80 K. In (a), the upper trace is a measure of the average intensity fluctuations of the probe pulses during the experiment. The semilog plot (b) shows the echo decay is exponential over a wide dynamic range. At 80 K the vibrational echo data give a value for the dephasing time constant of $T_2 = 25$ ps. Combining this with a pump-probe measurement of $T_1 = 18$ ps, a pure dephasing time constant of $T_2^* = 85$ ps was determined[81] at this temperature.

tion of a protein, the A_1 state of Mb-CO in glycerol : water.[82,83] Figure 12(a) shows echo decay data at 80 K. The horizontal trace at top is a monitor of the FEL pulse stability, obtained using the probe IR detector shown in Figure 5. A semilog plot in Figure 12(b) shows that the echo decay is fit by a single exponential over a wide dynamic range.

At 80 K, the vibrational echo data gives a value for the dephasing time constant of $T_2 = 25$ ps, corresponding to a Lorentzian homogeneous line 0.4 cm^{-1} wide, as compared to the absorption linewidth of $\sim$ 10 cm^{-1} at this temperature. At 80 K, the pump-probe experiment gives $T_1 = 18$ ps. Equation 2 can be used to compute a pure dephasing time constant of $T_2^* = 85$ ps. Thus, at 80 K pure dephasing is roughly five times slower than VR. Our temperature-dependent studies show that when temperature is increased from 80 to 300 K, the echo decay rate increases substantially.[82,83] Because the VR lifetime changes very slowly in this temperature range (cf. Fig. 8), these measurements indicate the temperature dependence of the pure dephasing process in Mb-CO is much steeper than the VR temperature dependence. The temperature dependence of the vibrational echo experiment will be described in more detail in other publications.[82,83]

Discussion of Echo Results

We have seen echoes throughout the 80–300 K temperature range, and at all these temperatures the echo decay is exponential in time. The existence of an echo signal yielding a homogeneous width ($1/\pi T_2$) narrower than the width of the absorption spectrum ($\Delta\nu$) provides definitive proof that the carbonyl vibrational transition is inhomogeneously broadened, even at ambient temperature. This result allows us to conclude that on the echo time scale, proteins exist in many different distinguishable conformational states which induce slightly different transition frequencies ($\Delta \sim 10$ cm^{-1}) of the carbonyl stretch.

The exponential echo decay proves the homogeneous lineshape is Lorentzian. Although this is the expected result for an ordered material such as a crystal, it need not be the case in a disordered system, as discussed elsewhere.[32] This result suggests the dynamic processes which cause pure dephasing are Markovian.[32] A Markovian process is one in which the dynamic behavior of the system at any time is independent of the past history of the system. Protein dynamics need not necessarily be Markovian. For example, the folding transition of a protein from a denatured state to a compact state is a non-Markovian process.

An extremely interesting interpretation of pure dephasing in Mb-CO is suggested by our VR studies. We found a correlation between the static frequency shift induced by the protein matrix and the rate of VR. The theory of pure dephasing developed by Kubo[30] treats the system as an oscillator with a time-dependent transition frequency $\omega(t)$ given by,

$$\omega(t) = \omega_0 + \Delta\Omega(t), \qquad (6)$$

where the $\Delta\Omega(t)$ term represents the time-dependent frequency fluctuations induced by the fluctuating forces. Pure dephasing is caused by fluctuations of the oscillator frequency. Since the magnitude of back-bonding is the primary determinant of the static frequency shift and the VR rate, it might be possible to show that fluctuations in back-bonding are the primary cause of pure dephasing. Since these fluctuations can be induced by the dynamical process of protein conformational relaxation, it should be possible to use vibrational echoes to investigate conformational dynamics in heme proteins. The VR experiments are sensitive to medium fluctuations only occurring on the very fast time scale of carbonyl oscillations ($\sim$ 20 fs). The echo measurements are, in addition, sensitive to medium fluctuations on picosecond and longer time scales, which is a time regime in which functionally important protein motions occur.[25]

CONCLUSIONS AND SUMMARY

In this article we have described how intense tunable mid-IR pulses have been used to study the dynamics of a ligand bound to the active site of a heme protein, myoglobin. We briefly described how the FEL at Stanford, a novel and extremely versatile new research tool, was used in two powerful and complementary experimental techniques, the pump-probe method of measuring absorption saturation recovery and the vibrational echo method of measuring optical dephasing. A brief outline of the quantum dynamic theoretical interpretation of these experimental methods was presented. The quantum mechanical force correlation function model for relaxation processes induced by fluctuations of the medium (porphyrin, protein, and solvent) was also discussed. A broad range of experimental results was presented, detailing studies where the molecular architecture and protein environment were systematically altered to provide information about the relationships between protein structure and active site dynamics.

The pump-probe method measures VR, the loss of energy from an excited carbonyl oscillator at the active site. There are many possible pathways in which one can imagine this energy transfer might take, but our experimental results show the dominant pathway involves anharmonic coupling from CO, through the π-bonded network of the porphyrin, to porphyrin vibrations with frequencies > 400 cm^{-1}. The through π-bond coupling mechanism explains the observed relationship between CO stretching frequency and VR rate. The most general conclusion of this study is that the heme protein influences molecular dynamics of bound ligands at the active site primarily via a passive mechanism where the protein electric field alters the through π-bond coupling between CO and heme, rather than an active mechanism in which different protein structures open up new channels for energy transfer from the ligand to the protein.

Our quite recent success with the vibrational echo technique is extremely encouraging. Echo measurements are sensitive to medium fluctuations on picosecond and longer time scales where functionally important protein conformational transitions exist. We have shown that on the echo time scale of $\sim$ 100 ps, proteins at and below ambient temperature exist in distinguishable conformational states characterized by slightly different carbonyl stretching frequencies. By combining pump-probe and echo measurements, we have deduced the existence of a temperature-dependent pure dephasing mechanism, which has a quite different temperature dependence than the VR process.

In some very recent work at the Stanford FEL Center, K. Peterson and C. Rella[84] have now shown it is possible to perform pump-probe experiments directly on the Mb protein itself. Using pulses tuned to 6.05 μm (1653 cm^{-1}), pump-probe experiments were performed on the amide I band-stretching band of Mb. VR lifetimes of roughly 1 ps were obtained. This new measurement demonstrates that pump-probe and photon echo studies of proteins need not be limited to ligands, but can be extended to protein backbone transitions, including those lower-frequency motions which might play an important role in protein function.

The extremely rapid development of new short-pulse laser sources in the mid-IR has already led to new tools for investigating fast time-scale protein dynamics. With each passing year, substantial improvements are being made in the areas of pulse energy, pulse duration, tunability, and ease of use. The application of these new sources to biospectroscopy, the development of powerful new experimental techniques to extract information from biomolecules, and the development of theoretical methods to understand this information present exciting new challenges to the biospectroscopy community.

This research was supported by the Medical Free Electron Laser Program, through the Office of Naval Research, by Contracts NOOO14-91-C-0170 and NOOO14-94-1-1024 (C.W.R., T.I.S., H.A.S., K.A.P., A.K., K.R., and M.D.F.). Additional support was provided by the Office of Naval Research, Biology Division, by Contract NOOO14-95-1-0259 (D.D.D. and J.R.H.). The authors acknowledge with gratitude the efforts of their valued collaborators, Professor Kenneth Suslick and Professor Steven Boxer, and their research groups.

REFERENCES

1. G. Vergoten, G. Fleury, and Y. Moscetto, "Low frequency vibrations of molecules with biological interest," in *Advances in Infrared and Raman Spectroscopy*, ed. by R. J. H. Clark and R. E. Hester, Heyden, Philadelphia, 1978, pp. 195–270.
2. F. Van De Ven, *Multidimensional NMR in Liquids*, VCH Publishers, New York, 1995.
3. A. G. Redfield and R. K. Gupta, "Pulsed-Fourier-transform nuclear magnetic resonance spectrometer," in *Advances in Magnetic Resonance*, ed. by J. S. Waugh, Academic Press, New York, 1971, pp. 82–116.

4. J. C. Owrutsky, M. Li, J. P. Culver, M. J. Sarisky, A. G. Yodh, and R. M. Hochstrasser, "Vibrational dynamics of condensed phase molecules studied by ultrafast infrared spectroscopy," in *Time Resolved Vibrational Spectroscopy VI,* ed. by A. Lau, Springer, New York, 1993, pp. 63–67.
5. J. C. Owrutsky, M. Li, B. Locke, and R. M. Hochstrasser, "Vibrational relaxation of the CO stretch vibration in hemoglobin-CO, myoglobin-CO, and protoheme-CO," *J. Phys. Chem.,* **99,** 4842–4846 (1995).
6. E. J. Heilweil, R. R. Casassa, R. R. Cavanaugh, and J. C. Stephenson, "Population lifetimes of OH (v = 1) and OD (v = 1) stretching vibrations of alcohols and silanols in dilute solution," *J. Chem. Phys.,* **85,** 5004 (1986).
7. E. J. Heilweil, R. R. Cavanagh, and J. C. Stephenson, "Population relaxation of CO (v = 1) vibrations in solution phase metal carbonyl complexes," *Chem. Phys. Lett.,* **134,** 181–188 (1987).
8. E. J. Heilweil, R. R. Cavanagh, and J. C. Stephenson, "CO (v = 1) population lifetimes of metal-carbonyl cluster compounds in dilute $CHCl_3$ solution," *J. Chem. Phys.,* **89,** 230–239 (1988).
9. E. J. Heilweil, J. C. Stephenson, and R. R. Cavanagh, "Measurements of CO (v = 1) population lifetimes: Metal-carbonyl cluster compounds supported on SiO_2," *J. Phys. Chem.,* **92,** 6099–6103 (1988).
10. E. J. Heilweil, R. R. Cavanagh, and J. C. Stephenson, "Picosecond study of the population lifetime of CO (v = 1) chemisorbed on SiO_2-supported rhodium particles," *J. Chem. Phys.,* **89,** 5342 (1988).
11. A. Tokmakoff, B. Sauter, and M. D. Fayer, "Temperature-dependent vibrational relaxation in polyatomic liquids: Picosecond infrared pump-probe experiments," *J. Chem. Phys.,* **100,** 9035 (1994).
12. A. Tokmakoff, D. Zimdars, B. Sauter, R. S. Francis, R. S. Kwok, and M. D. Fayer, "Vibrational photon echoes in a liquid and glass–room temperature to 10 K," *J. Chem. Phys.,* **101,** 1741–1744 (1994).
13. A. Tokmakoff, D. Zimdars, R. S. Urdahl, R. S. Francis, A. S. Kwok, and M. D. Fayer, "Infrared vibrational photon echo experiments in glasses," *J. Phys. Chem.,* **99,** 13310–13320 (1995).
14. A. Tokmakoff and M. D. Fayer, "Infrared photon echo experiments—exploring vibrational dynamics in liquids and glasses," *Acc. Chem. Res.,* **28,** 437–445 (1995).
15. A. Tokmakoff, A. Kwok, U. Urdahl, D. A. Zimdars, R. Francis, and M. D. Fayer, "Vibrational dynamics of liquids and glasses probed with IR photon echoes," *Laser Phys.,* **5,** 652–655 (1995).
16. A. Tokmakoff and M. D. Fayer, "Homogeneous vibrational dynamics and inhomogeneous broadening in glass-forming liquids–infrared photon echo experiments from room temperature to 10 K," *J. Chem. Phys.,* **103,** 2810–2826 (1995).
17. A. Tokmakoff, A. S. Kwok, R. S. Urdahl, R. S. Francis, and M. D. Fayer, "Multilevel vibrational dephasing and vibrational anharmonicity from infrared photon echo beats," *Chem. Phys. Lett.,* **234,** 289–295 (1995).
18. D. D. Dlott and M. D. Fayer, "Applications of infrared free-electron lasers: Basic research on the dynamics of molecular systems," *IEEE J. Quantum Electron.,* **27,** 2697–2713 (1991).
19. Y. S. Bai, S. R. Greenfield, M. D. Fayer, T. I. Smith, J. C. Frisch, R. L. Swent, and H. A. Scwettman, "Picosecond photon echo experiments using a superconducting accelerator pumped free electron laser," *J. Opt. Soc. Am. B,* **8,** 1652–1656 (1991).
20. A. Tokmakoff, C. D. Marshall, and M. D. Fayer, "Optical parametric amplification of 1-kHz high-energy picosecond midinfrared pulses and application to infrared transient-grating experiments on diamond," *J. Opt. Soc. Am. B,* **10,** 1785–1791 (1993).
21. F. Seifert, V. Petrov, and M. Woerner, "Solid-state laser system for the generation of midinfrared femtosecond pulses tunable from 3.3 to 10 μ," *Opt. Lett.,* **19,** 2009–2011 (1994).
22. F. Yang and G. N. Phillips, "Structures of CO-, deoxy-, and met-myoglobins at various pH values," *J. Mol. Biol.,* **256,** 762–774 (1996).
23. W. S. Caughey, H. Shimada, M. G. Choc, and M. P. Tucker, "Dynamic protein structures: Infrared evidence for four discrete rapidly interconverting conformers at the carbon monoxide binding site of bovine heart myoglobin," *Proc. Natl. Acad. Sci. USA,* **78,** 2903–2907 (1981).
24. A. Ansari, J. Berendzen, D. Braunstein, B. R. Cowen, H. Frauenfelder, M. K. Hong, I. E. T. Iben, J. B. Johnson, P. Ormos, T. B. Sauke, R. Scholl, A. Schulte, P. J. Steinbach, J. Vittitow, and R. D. Young, "Rebinding and relaxation in the myoglobin pocket," *Biophys. Chem.,* **26,** 337–355 (1987).
25. A. Ansari, E. E. DiIorio, D. D. Dlott, H. Frauenfelder, I. E. T. Iben, P. Langer, H. Roder, T. B. Sauke, and E. Shyamsunder, "Ligand binding to heme proteins: Relevance of low-temperature data," *Biochemistry,* **25,** 3139–3146 (1986).
26. A. P. Thorne, *Spectrophysics,* Chapman and Hall, London, 1974.
27. N. A. Kurnit, I. D. Abella, and S. R. Hartmann, "Observation of a photon echo," *Phys. Rev. Lett.,* **13,** 567–568 (1964).
28. A. Laubereau and W. Kaiser, "Vibrational dynamics of liquids and solids investigated by picosecond light pulses," *Rev. Mod. Phys.,* **50,** 607–665 (1978).
29. P. W. Anderson, "Exchange narrowing in paramegnetic resonance," *Rev. Mod. Phys.,* **25,** 269–276 (1953).
30. R. Kubo and K. Tomita, "A general theory of magnetic resonance absorption," *J. Phys. Soc. Jpn.,* **9,** 888–919 (1954).
31. B. DiBartolo, *Optical Interactions in Solids,* Wiley, New York, 1968.
32. M. Berg, C. A. Walsh, L. R. Narasimhan, K. A. Lit-

tau, and M. D. Fayer, "Dynamics in low temperature glasses: Theory and experiments on optical dephasing, spectral diffusion, and hydrogen tunneling," *J. Chem. Phys.*, **88,** 1564–1587 (1988).
33. Y. S. Bai and M. D. Fayer, "Time scales and optical dephasing measurements: Investigation of dynamics in complex systems," *Phys. Rev. B.*, **39,** 11066–11084 (1989).
34. L. R. Narasimham, K. A. Littau, D. W. Pack, Y. S. Bai, A. Elschner, and M. D. Fayer, "Probing organic glasses at low temperature with variable time scale optical dephasing measurements," *Chem. Rev.*, **90,** 439–457 (1990).
35. D. S. Anex and G. E. Ewing, "Transfer and storage of vibrational energy in liquids: Collisional uppumping of carbon monoxide in liquid argon," *J. Phys. Chem.*, **90,** 1604–1610 (1986).
36. R. Disselkamp and G. E. Ewing, "High vibrational states of carbon monoxide in liquid argon: Overtone intensity enhancement and reactions with oxygen," *J. Phys. Chem.*, **93,** 6334–6339 (1989).
37. N. Legay-Sommaire and F. Legay, "Analysis of the infrared emission and absorption spectra from isotopic CO molecules in solid α-CO," *Chem. Phys.*, **66,** 315–325 (1982).
38. P. Moore, A. Tokmakoff, T. Keyes, and M. D. Fayer, "The low frequency density of states and vibrational population dynamics of polyatomic molecules in liquids," *J. Chem. Phys.*, **103,** 3325–3334 (1995).
39. R. R. Cavanagh, J. D. Beckerle, M. P. Casassa, E. J. Heilweil, and J. C. Stephenson, "Subpicosecond probing of vibrational energy transfer at surfaces," *Surf. Sci.*, **269/270,** 113–119 (1992).
40. R. R. Cavanagh, E. J. Heilweil, and J. C. Stephenson, "Time-resolved probes of surface dynamics," *Surf. Sci.*, **283,** 226–232 (1993).
41. R. R. Cavanagh, E. J. Heilweil, and J. C. Stephenson, "Time-resolved measurements of energy transfer at surfaces," *Surf. Sci.*, **299/300,** 643–655 (1994).
42. J. R. Hill, D. D. Dlott, M. D. Fayer, K. A. Peterson, C. W. Rella, M. M. Rosenblatt, K. S. Suslick, and C. Ziegler, "Vibrational relaxation of carbon monoxide in model heme compounds: 6-coordinate metalloporphyrins (M = Fe, Ru, Os)," *Chem. Phys. Lett.*, **244,** 218–223 (1995).
43. R. M. Hochstrasser, "Femtosecond infrared probing of biomolecules," in *Proc. SPIE-Int. Soc. Opt. Eng. (Laser Spectroscopy of Biomolecules)*, 1992, pp. 16–28.
44. M. Gomez and J. C. Tully, "Electronic and phonon mechanisms of vibrational relaxation: CO on Cu(100)," *J. Vac. Sci. Technol. A*, **11,** 1914–1920 (1993).
45. M. Head-Gordon and J. C. Tully, "Vibrational relaxation on metal surfaces: Molecular-orbital theory and application to CO/Cu(100)," *J. Chem. Phys.*, **96,** 3939–3949 (1992).
46. M. Sassaroli and D. L. Rousseau, "Simulation of carboxymyoglobin photodissociation," *J. Biol. Chem.*, **261,** 16292–16294 (1986).
47. E. R. Henry, M. Levitt, and W. A. Eaton, "Molecular dynamics simulation of photodissociation of carbon monoxide from hemoglobin," *Proc. Natl. Acad. Sci. USA*, **82,** 2034–2038 (1985).
48. E. R. Henry, W. A. Eaton, and R. M. Hochstrasser, "Molecular dynamics simulations of cooling in laser-excited heme proteins," *Proc. Natl. Acad. Sci. USA*, **83,** 8982–8986 (1986).
49. A. Roitberg, R. B. Gerber, R. Elber, and M. A. Ratner, "Anharmonic wave functions of proteins: Quantum self-consistent field calculations of BPTI," *Science*, **268,** 1319–1322 (1995).
50. V. M. Kenkre, A. Tokmakoff, and M. D. Fayer, "Theory of vibrational relaxation of polyatomic molecules in liquids," *J. Chem. Phys.*, **101,** 10618–10629 (1994).
51. R. Varadarajan, A. Szabo, and S. G. Boxer, "Cloning, expression in *Escherichia coli*, and reconstitution of human myoglobin," *Proc. Natl. Acad. Sci. USA*, **82,** 5681–5684 (1985).
52. B. A. Springer and S. G. Sligar, "High-level expression of sperm whale myoglobin in *Escherichia coli*," *Proc. Natl. Acad. Sci. USA*, **84,** 8961–8965 (1987).
53. C. A. Brau, "Free-electron lasers," *Science*, **239,** 1115–1121 (1988).
54. H. A. Schwettman, T. I. Smith, and R. L. Swent, "The Stanford FEL Center," *Nucl. Instr. Methods*, **A341,** 19 (1994).
55. S. R. Greenfield, Y. S. Bai, and M. D. Fayer, "Optical dephasing of a near infrared dye in PMMA: Photon echoes using the superconducting accelerator pumped free electron laser," *Chem. Phys. Lett.*, **170,** 133–138 (1990).
56. S. L. Shapiro, *Ultrashort Light Pulses*, Springer-Verlag, Berlin, 1977.
57. K. W. Berryman, B. A. Richman, H. A. Schwettman, T. I. Smith, and R. L. Swent, "FEL Center user diagnostics and control," *Nucl. Instr. Methods*, **A358,** 300–303 (1995).
58. A. Marziali and T. I. Smith, "Demonstration of wavelength stabilization in a free electron laser," *IEEE J. Quantum Electron.*, **30,** 2185–2187 (1994).
59. D. D. Dlott and M. D. Fayer, "Application of a two-color free-electron laser to condensed-matter molecular dynamics," *J. Opt. Soc. Am. B*, **6,** 977–994 (1989).
60. J. R. Hill, D. D. Dlott, C. W. Rella, K. A. Peterson, S. M. Decatur, S. G. Boxer, and M. D. Fayer, "Vibrational dynamics of carbon monoxide at the active sites of mutant heme proteins," *J. Phys. Chem.*, **100,** 12100–12107 (1996).
61. J. R. Hill, A. Tokmakoff, K. A. Peterson, B. Sauter, D. Zimdars, D. D. Dlott, and M. D. Fayer, "Vibrational dynamics of carbon monoxide at the active site of myoglobin: picosecond infrared free-electron

laser pump-probe experiments," *J. Phys. Chem.*, **98,** 11213–11219 (1994).
62. R. L. Bohon and W. T. Conway, "DTA studies on the glycerol-water system," *Thermochim. Acta,* **4,** 321–341 (1972).
63. S. Balasubramanian, D. G. Lambright, and S. G. Boxer, "Perturbations of the distal heme pocket in human myoglobin mutants probed by infrared spectroscopy of bound CO: Correlation with ligand binding kinetics," *Proc. Natl. Acad. Sci. USA,* **90,** 4718–4722 (1993).
64. S. M. Decatur and S. G. Boxer, "A test of the role of electrostatic interactions in determining the CO stretch frequency in carbonmonoxymyoglobin," *Biochem. Biophys. Res. Commun.,* **212,** 159–164 (1995).
65. S. M. Decatur and S. G. Boxer, "1H NMR characterization of myoglobins where exogenous ligands replace the proximal histidine," *Biochemistry,* **34,** 2122–2129 (1995).
66. R. E. Dickerson and I. Geis, *Hemoglobin: Structure, Function, Evolution, and Pathology,* Benjamin/Cummings. Menlo Park, CA, 1983.
67. J. R. Hill, C. J. Ziegler, K. S. Suslick, D. D. Dlott, C. W. Rella, and M. D. Fayer, "Tuning the vibrational relaxation of CO bound to heme and porphyrin complexes," *J. Phys. Chem.* (in press).
68. D. W. Oxtoby, "Vibrational population relaxation in liquids," in *Advances in Chemical Physics,* eds. J. Jortner, R. D. Levine, S. A. Rice, **47,** 1981, pp. 487–519.
69. T. M. Wu and R. F. Loring, "Phonons in liquids: A random walk approach," *J. Chem. Phys.,* **97,** 8568–8575 (1992).
70. B.-C. Xu and R. M. Stratt, "Liquid theory for band structure in a liquid. II. p orbitals and phonons," *J. Chem. Phys.,* **92,** 1923–1935 (1990).
71. G. Seeley and T. Keyes, "Normal-mode analysis of liquid-state dynamics," *J. Chem. Phys.,* **91,** 5581–5586 (1989).
72. B. A. Springer, S. G. Sligar, J. S. Olson, and G. N. Phillips, Jr., "Mechanisms of ligand recognition in myoglobin," *Chem. Rev.,* **94,** 699–714 (1994).
73. X. Y. Li and T. G. Spiro, "Is bound CO linear or bent in heme proteins? Evidence from resonance Raman and infrared spectroscopic data," *J. Am. Chem. Soc.,* **110,** 6024–6033 (1988).
74. S. Hu, K. M. Vogel, and T. G. Spiro, "Deformability of heme protein CO adducts: FT-IR assignment of the FeCO bending mode," *J. Am. Chem. Soc.,* **116,** 11187–11188 (1994).
75. M. Lim, T. A. Jackson, and P. A. Anfinrud, "Carbonmonoxide binds to myoglobin from a heme pocket docking site to form nearly linear Fe-C-O," *Science,* **269,** 962 (1995).
76. D. Ivanov, J. T. Sage, M. Keim, J. R. Powell, S. A. Asher, and P. M. Champion, "Determination of CO orientation in myoglobin by single-crystal IR linear dichroism," *J. Am. Chem. Soc.,* **116,** 4139–4140 (1994).
77. I. Benjamin and W. P. Reinhardt, "A quantum theoretic model of vibrational relaxation of a diatomic molecule adsorbed on a surface," *J. Chem. Phys.,* **90,** 7535–7541 (1989).
78. F. A. Cotton and G. Wilkinson. *Advanced Inorganic Chemistry,* Wiley-Interscience, New York, 1988.
79. G. B. Ray, X.-Y. Li, J. A. Ibers, J. L. Sessler, and T. G. Spiro, "How far can proteins bend the FeCO unit? Distal polar and steric effects in heme proteins and models," *J. Am. Chem. Soc.,* **116,** 162–176 (1994).
80. R. Elber and M. Karplus, "Multiple conformational states of proteins: A molecular dynamics analysis of myoglobin," *Science,* **235,** 318–321 (1987).
81. R. H. Austin, K. W. Beeson, L. Eisenstein, H. Frauenfelder, and I. C. Gunsalus, "Dynamics of ligand binding to myoglobin," *Biochemistry,* **14,** 5355–5373 (1975).
82. C. W. Rella, A. Kwok, K. D. Rector, J. R. Hill, H. A. Schwettman, D. D. Dlott, and M. D. Fayer, "Vibrational echo studies of protein dynamics," *Phys. Rev. Lett.,* **77,** pp. 1648–1651 (1996).
83. C. W. Rella, A. Kwok, K. D. Rector, J. R. Hill, H. A. Schwettman, D. D. Dlott, and M. D. Fayer, "Picosecond infrared vibrational echo studies of CO-myoglobin," *J. Phys. Chem.,* **100,** 15620–15629 (1996).
84. C. W. Rella and K. A. Peterson (unpublished).

Received January 24, 1996
Revised March 22, 1996
Accepted July 2, 1996